The Astronomical Journal, 159:198 (16pp), 2020 May https://doi.org/10.3847/1538-3881/ab7cce

Cataclysmic Variables in the First Year of the Zwicky Transient Facility

Paula Szkody[1], Brooke Dicenzo[1], Anna Y. Q. Ho[2], Lynne A. Hillenbrand[2], Jan van Roestel[2], Margaret Ridder[1], Isabel DeJesus Lima[1,3], Melissa L. Graham[4], Eric C. Bellm[1], Kevin Burdge[2], Thomas Kupfer[5], Thomas A. Prince[2], Frank J. Masci[6], Przemyslaw J. Mróz[2], V. Zach Golkhou[7,8], Michael Coughlin[9], Virginia A. Cunningham[10], Richard Dekany[11], Matthew J. Graham[2], David Hale[11], David Kaplan[12], Mansi M. Kasliwal[2], Adam A. Miller[13], James D. Neill[2], Maria T. Patterson[14], Reed Riddle[2], Roger Smith[2], and Maayane T. Soumagnac[15,16]

[1] University of Washington, Department of Astronomy, Box 351580, Seattle, WA 98195, USA; szkody@astro.washington.edu
[2] Division of Physics, Mathematics and Astronomy, California Institute of Technology, Pasadena, CA 91125, USA
[3] Instituto Nacional de Pesquisas Espaciais (INPE/MCTIC), Av. dos Astronautas, 1758 Sao Jose dos Campos, Brazil
[4] DIRAC Institute, University of Washington, Department of Astronomy, Box 351580, Seattle, WA 98195, USA
[5] Kavli Institute for Theoretical Physics, University of California Santa Barbara, Santa Barbara, CA, USA
[6] IPAC, California Institute of Technology, Pasadena, CA 91125, USA
[7] University of Washington Department of Astronomy, University of Washington, Box 351580 Seattle, WA 98195, USA
[8] The eScience Institute, University of Washington, Seattle, WA 98195, USA
[9] LIGO Laboratory, California Institute of Technology, Pasadena, CA 91125, USA
[10] Department of Astronomy, University of Maryland, College Park, MD 20742, USA
[11] Caltech Optical Observatories, California Institute of Technology, Pasadena, CA 91125, USA
[12] Department of Physics, University of Wisconsin-Milwaukee, Milwaukee, WI 53201, USA
[13] Department of Physics and Astronomy, Northwestern University, Evanston, IL 60208, USA
[14] High Alpha, 55 Monumnet Circle Suite 1400, Indianapolis, IN 46204, USA
[15] Lawrence Berkeley National Lab, 1 Cyclotron Road, Berkeley, CA 94720, USA
[16] Department of Particle Physics and Astrophysics, Weizmann Institute of Science, Rehovot, Israel

Received 2019 December 10; revised 2020 February 4; accepted 2020 February 16; published 2020 April 10

Abstract

Using selection criteria based on amplitude, time, and color, we have identified 329 objects as known or candidate cataclysmic variables (CVs) during the first year of testing and operation of the Zwicky Transient Facility. Of these, 90 are previously confirmed CVs, 218 are strong candidates based on the shape and color of their light curves obtained during 3–562 days of observation, and the remaining 21 are possible CVs but with too few data points to be listed as good candidates. Almost half of the strong candidates are within 10 deg of the galactic plane, in contrast to most other large surveys that have avoided crowded fields. The available Gaia parallaxes are consistent with sampling the low mass transfer CVs, as predicted by population models. Our follow-up spectra have confirmed Balmer/helium emission lines in 27 objects, with four showing high-excitation He II emission, including candidates for an AM CVn, a polar, and an intermediate polar. Our results demonstrate that a complete survey of the Galactic plane is needed to accomplish an accurate determination of the number of CVs existing in the Milky Way.

Unified Astronomy Thesaurus concepts: Astronomical object identification (87); Compact binary stars (283); Spectroscopy (1558); Dwarf novae (418)

Supporting material: machine-readable tables

1. Introduction

The Zwicky Transient Facility (ZTF) is a northern all-sky survey that uses the Palomar 48 inch telescope equipped with a 47 deg^2 field-of-view camera (Bellm et al. 2019a, 2019b; Graham et al. 2019; Masci et al. 2019). The advantages of the ZTF survey compared to past and ongoing northern sky surveys are the combination of large sky coverage that includes the Galactic plane, along with color information and increased temporal coverage, and the availability of nightly alerts. These aspects are ideal for finding variable stars, especially those that have non-periodic, erratic brightness changes such as cataclysmic variables (CVs), which consist of close binaries with mass transfer from a late main-sequence secondary to a white dwarf (see Warner 1995 for a review of all types of CVs). Combining the results from all-sky surveys along with astrometric data from Gaia will lead to the correct number and density of CVs throughout our Galaxy, thus ultimately constraining population models and close binary evolution scenarios.

The ZTF project uses 40% of the time for the public, 40% for partnerships, and 20% for Caltech. As part of the public portion, the available sky is sampled in ZTF g or r filters every three nights and the available Galactic plane with $|b| \leqslant 7°$ every night in both g and r with mean 5σ limiting magnitudes of 21 and saturation near 15 mag. Alerts on all variable objects are available every night. Commissioning took place in the latter part of 2017 with the official start of the 3 yr survey on 2018 March 18 and the first public data release DR1 occurred on 2019 May 8. DR1 is available from IPAC.[17]

The alerts are constructed from difference images between a reference field (consisting of a minimum of 15 images) and the new field. These alerts pass through the GROWTH Marshal (Kasliwal et al. 2019), which uses various filters constructed by participants to select specific types of variables and transients. One such filter was created to select candidate CVs. In the CVs with a non-magnetic white dwarf ($B < 1$ MG), the mass transfer accumulates in a disk before accreting onto the white

[17] https://www.ipac.caltech.edu/project/ztf

dwarf. The amount of mass transfer and accretion determines what the light curve of a specific CV will look like. Those with relatively low transfer rate values will undergo a disk instability that results in a dwarf nova outburst (a rise in brightness of 2–9 mag within 1–3 days, the high brightness lasting for 1–15 days, and a subsequent return to quiescence), with a repetition timescale of weeks to months. The lowest mass transfer systems are those with the largest amplitudes, the longest times at outburst, and the longest recurrence time between outbursts (years). The highest rates of mass transfer result in nova-like (NL) systems, which have no outbursts but sometimes undergo several magnitude transitions between low and high accretion states that can last for weeks at a time. In systems with a magnetic white dwarf, the inner disk region can be channeled to the magnetic poles via accretion curtains (called intermediate polars, IPs) or in the highest field cases (termed polars), the mass transfer goes directly to the white dwarf magnetic poles, and no disk exists. Without a disk, there are no outbursts but high and low states of accretion can occur, resulting in several magnitude changes in their light curves on timescales of weeks. The colors of CVs are generally blue (ZTF $g - r$ close to 0 and even bluer during an outburst) due to the contributions of the hot white dwarf and the accretion disk. However, long-period systems with K-type secondaries or those with magnetic white dwarfs and resulting cyclotron emission from the accretion pole can be redder in color.

To find CVs, a simple GROWTH filter was used to search for non-moving point sources with an amplitude change of 2 mags within a time span of 3 days and a color (from PanSTARRS) of $g - r < 0.6$. A real-bogus (rb) filter (calibrated from a zooniverse program of human classification on a large data set of ZTF images) was set to be low (0.1) to maximize findings. The filter began its full operation on 2018 June 5. With this filter, each night resulted in anywhere from 30 to 200 objects, the number mostly dependent on the weather and partly on the location of the observed fields. The resulting objects were then searched by eye to identify possible CVs. After many months of data, it became clear that it was most worthwhile to do the eye search if the rb was greater than 0.5. Future refinements to the filter and machine-learning classifiers being developed by other teams in the ZTF project will undoubtedly be able to decrease the amount of human interaction required. This paper presents the resulting previously confirmed CVs and CV candidates found using the simple GROWTH Marshal filter up to the time of the first public data release.

2. Identifying CVs

Each night, the combined g, r ZTF light curves of the filtered objects provided by the Marshal were scanned by eye to determine a possible dwarf nova outburst or a change in state of an NL system within the 30 day interval depicted by the Marshal. Likely candidates were saved and checked against known sources via SIMBAD, the Sloan Digital Sky Survey (York et al. 2000), the Catalina Real-time Transient Survey (CRTS; Drake et al. 2009, 2014; Breedt et al. 2014), Mobile Astronomical System of TElescopic Robots (MASTER; Lipunov et al. 2010), and All-Sky Automated Survey for Supernovae (ASAS-SN; Shappee et al. 2014). The saved sources continued to be monitored to help determine the correct classification. In many cases, this allowed full outbursts to be observed, in other cases, only rises or declines from an outburst or a high/low state were viewed. Other ZTF groups also transferred objects that passed their different filters (e.g., nuclear transients, SN, etc.) if they thought they might be CVs. When the weather allowed long stretches of good observations, it was common to end with 50–70 previously known CVs and/or good candidates per month. The most frequent contaminants were RR Lyrae and other large amplitude periodic variables that fell within the color range.

Follow-up spectra on some objects were obtained using several telescopes, sometimes with multiple spectra on the same object (27 systems with the Palomar 60-in, 5 with the Palomar 200-in, 10 with the Keck I0 m, 4 with the William Herschel 4.2 m (WHT), 14 with the Apache Point Observatory (APO) 3.5 m, and 2 with the Liverpool 2 m telescope) to confirm candidates. The presence of Balmer emission (from the decline or quiescent state) or the presence of He II emission (indicative of a magnetic white dwarf or a very high mass transfer system) were used as confirmation criteria. Spectra obtained too close to an outburst generally showed only Balmer absorption lines and are indicative of an accretion disk but were not used as confirmation.

The Spectral Energy Distribution Machine (SEDM; Blagorodnova et al. 2018; Rigault et al. 2019), a low-resolution (50 Å) integral field spectrograph operating from 3650 to 10000 Å, obtained spectra on the Palomar 60-in telescope. An automatic pipeline reduced the data and uploaded it to the Marshal. The Double Beam Spectrograph (Oke & Gunn 1982) was used on the Palomar 200 in, the Low Resolution Imaging Spectrometer (LRIS; Oke et al. 1995) on the Keck, and the Spectrograph for the Rapid Acquisition of Transients (SPRAT) on the Liverpool telescope (Steele et al. 2004), and uploaded after reduction pipelines. A few spectra were obtained at medium resolution (3.3 Å) with the WHT using the Auxiliary-port CAMera (ACAM) spectrograph (Benn et al. 2008). The APO data were obtained with the Double Imaging Spectrograph using either low-resolution (2 Å) or high-resolution (0.6 Å) gratings to cover the Balmer lines and the data reduced using IRAF routines to calibrate the data via He, Ne, and Ar lamps and flux standards obtained during each night. The APO blue CCD suffered contamination problems throughout the year, so most of the data collected were only from the red side of the dichroic (5500–9000 Å).

3. Results

The year-long scans of the GROWTH Marshal with the CV filter yielded 90 previously confirmed (from spectra or from the presence of a superhump outburst feature; Warner 1995) CVs, 218 strong candidates based on their light curves, and 21 objects that might be CVs but the data are too limited to tell for sure. Table 1 lists the previously confirmed objects, Table 2 the strong candidates, and Table 3 the remaining possibilities. Some sources were listed as candidates in CRTS or MASTER, but if they have not been confirmed, we placed them in Table 2. In the rest of this paper, we will generally refer to objects by their abbreviated R.A.(HHMM) and decl.(Deg) i.e., ZTF0014+59, but provide R.A.(HHMMSS) if needed to differentiate sources. The tables also provide the Galactic latitude, the range in magnitudes from outburst peak to quiescence, or from high-to-low accretion states observed by ZTF, the Gaia parallax and errors in mas (for those objects with a measurement that was more than three times the error), the number of normal outbursts and longer superoutbursts (SOBs) observed in the

Table 1
Known Confirmed CVs

ZTF	R.A.	Decl.	$b°$	Δmag	p(mas)	Out	Days	SDSS	CRTS	Spec[a]	ID and Other Surveys[b]
17aaaemzh	00 15 38.27	+26 36 56.5	−35.6	13.8–21.7	1.64 ± 0.19	1	125	Y	Y3	SD	AT2016eav,G
18abdlywu	00 38 54.83	+61 13 00.2	−1.6	14.3–20.5	1.79 ± 0.26	2	224	⋯	⋯	⋯	KP Cas,G
18abgopgb	01 07 03.88	+42 43 12.0	−20.1	15.5–20.0	1.06 ± 0.25	SOB	315	Y	Y3	AP	IZ And,AT2018akr,G
17aaawpsz	02 13 15.49	+53 38 22.8	−7.3	16.8–20.0	⋯	2	137	⋯	⋯	⋯	MOT,Gx,Atel5536,K,G
18acgplgw	02 50 00.20	+37 39 22.1	−19.5	14.3–20.6	1.99 ± 0.11	4	153	⋯	Y3	⋯	PY Per,G
18aabeymw	03 20 15.29	+44 10 59.1	−11.0	15.3–20.9	2.11 ± 0.24	SOB	143	Y	⋯	⋯	USNO,K,G
18abtmzoi	04 06 59.82	+00 52 43.7	−35.3	15.4–20.8	1.78 ± 0.20	1	179	Y	Y3	⋯	CBET1463,G
17aaaslud	04 08 34.99	+51 14 48.1	−0.4	13.7–21.0	1.71 ± 0.05	6	250	Y	⋯	⋯	FO Per,G
17aaarlrs	04 09 12.17	+48 22 06.2	−2.5	16.2–20.3	1.11 ± 0.11	11	230	⋯	⋯	⋯	MY Per
18abscxct	04 23 32.91	+74 52 50.2	17.5	13.3–20.2	3.52 ± 0.11	SOB	223	⋯	⋯	⋯	HamburgSurvey,G
17aaacdos	04 53 16.88	+38 16 28.4	−3.6	15.0–19.0	1.69 ± 0.34	7	233	⋯	⋯	⋯	HV Aur,G
17aacucfy	05 01 24.15	+20 38 17.7	−12.9	15.8–20.2	1.84 ± 0.21	5	163	⋯	Y3	AP	ATel2266,G
17aaavfwx	05 06 13.12	−04 08 07.7	−25.2	13.3–20.1	2.66 ± 0.12	2	124	Y	Y3	⋯	AQ Eri,G
17aadaxwu	05 47 48.38	+28 35 10.9	0.2	14.1–16.5	1.83 ± 0.07	1	3	⋯	⋯	⋯	FS Aur,G
18abwsres	05 58 45.48	+39 15 33.0	7.6	14.2–19.0	1.81 ± 0.25	SOB,1	237	⋯	⋯	⋯	USNO,AT2016ggz,K,G
17aacpcfv	06 12 04.47	+25 28 32.6	3.4	17.2–20.0	⋯	2	327	Y	⋯	⋯	HQ Gem,AT2017gbf,G
17aadnmap	06 15 43.92	+28 35 08.4	5.6	16.6–20.0	2.29 ± 0.39	HL	68	⋯	⋯	⋯	KR Aur,G
17aacklbl	06 16 43.23	+15 24 11.2	−0.5	13.2–20.0	2.02 ± 0.11	8	541	⋯	⋯	⋯	CZ Ori,G
18aaahnyx	07 18 03.34	+64 47 44.7	27.2	15.3–18.2	1.57 ± 0.16	1	217	Y	Y2	AP	MOT,AT2018hzr,PTF,G
18aagqdbp	07 44 19.75	+32 54 48.2	24.8	17.8–20.3	⋯	2	480	Y	Y4	⋯	AM CVn type,G
18aaicnwh	07 50 59.97	+14 11 50.2	19.5	15.9–20.3	1.32 ± 0.28	2	411	Y	Y3	SD	MOT,G
17aacbiid	07 51 07.52	+30 06 28.2	25.3	15.1–20.6	⋯	2	300	Y	Y2	⋯	K,G
17aacplzj	07 56 48.05	+30 58 05.0	26.7	16.8–20.4	⋯	SOB	87	Y	Y3	SD	G
17aabyrpg	08 08 46.20	+31 31 05.9	29.3	14.2–20.8	⋯	2	556	Y	Y7	SD	PTF,G
18aacluoi	08 16 10.82	+45 30 10.1	33.4	15.9–20.3	⋯	2	470	Y	Y3	SD	AAVSO,G
18aaadlpa	08 54 14.01	+39 05 36.7	39.8	16.2–19.3	1.82 ± 0.38	HL	472	Y	HL	SD	FR Lyn,G
18aaacmsd	09 43 25.89	+52 01 28.8	47.1	15.2–20.6	1.21 ± 0.26	5	346	Y	Y2	SD	G
17aaapome	10 05 15.37	+19 11 07.9	51.2	13.0–19.7	2.57 ± 0.24	3	411	Y	Y2	SD	2MASS,G
18abcsatf	10 18 12.99	+71 55 42.9	40.6	14.4–20.5	⋯	3	326	⋯	⋯	⋯	CI UMa,G
17aacldol	10 19 47.24	+33 57 53.3	56.8	14.9–20.4	1.37 ± 0.25	2	562	Y	Y3	SD	AC LMi,G
18aaadhmx	10 43 56.60	+58 07 31.4	51.8	15.8–20.8	⋯	2	384	Y	⋯	SD	IY UMa
17aaajlbs	10 54 30.51	+30 06 09.1	64.2	14.3–18.7	3.08 ± 0.12	4	562	Y	Y2	SD	SX LMi,G
17aaajlfw	11 05 39.78	+25 06 28.0	66.2	14.0–19.3	8.83 ± 0.08	HL	532	Y	HL	SD	ST LMi,G
18aaadcme	11 35 51.07	+53 22 46.2	60.3	15.1–20.6	⋯	4	416	Y	⋯	SD	G
18aaadclg	11 57 44.85	+48 56 17.9	65.8	15.2–20.7	0.60 ± 0.03	⋯	480	Y	Y	SD	BE UMa(pre-CV)
18aajoejk	12 27 40.85	+51 39 24.7	65.1	15.1–20.8	2.75 ± 0.20	2	397	Y	Y4	SD	USNO,G
19aaqhcmn	12 32 25.77	+14 20 41.7	76.5	13.4–20.6	⋯	SOB	103	Y	⋯	⋯	AL Com,G
18aambkqd	13 05 14.74	+58 28 56.2	58.6	16.9–20.9	⋯	5	410	Y	Y3	SD	G
18aalrikz	13 07 53.84	+53 51 30.3	63.1	15.8–20.9	1.51 ± 0.12	HL	408	Y	Y4	SD	EV UMa,G
18aautxxk	14 11 18.31	+48 12 57.6	63.8	13.0–19.5	2.36 ± 0.30	SOB	410	Y	Y3	K,AP	AM CVn type
18abfyzmf	14 25 48.07	+15 15 01.2	65.1	17.1–20.8	⋯	2	324	Y	Y2	⋯	K
18aagsgqc	14 57 44.75	+40 43 40.5	60.7	12.8–21.0	1.47 ± 0.20	2	312	⋯	Y2	⋯	TT Boo,G
18abaulyr	15 34 12.18	+59 48 31.8	47.2	14.8–20.0	1.74 ± 0.43	1	31	Y	Y1	⋯	DM Dra,G
18aaisedb	15 51 22.39	+71 45 11.6	39.1	15.0–19.8	1.89 ± 0.05	18	409	⋯	⋯	⋯	SS UMi,G
18adbahiw	15 56 44.23	−00 09 50.4	37.8	14.5–19.3	3.24 ± 0.21	1	125	Y	Y3	SD	V493 Ser,AT2018hbm,G
18aaomiig	16 00 03.71	+33 11 13.7	49.1	14.1–20.0	⋯	SOB,1	389	Y	Y12	⋯	VW CrB,G
18abjzbhm	16 04 19.02	+16 15 48.3	44.2	17.5–20.0	1.10 ± 0.27	1	308	Y	Y5	SD	MNRAS,G
18aauxwft	16 19 35.80	+52 46 31.6	44.0	16.3–21.0	2.28 ± 0.23	HL	383	Y	Y2	SD	2MASS,G

Table 1
(Continued)

ZTF	R.A.	Decl.	$b°$	Δmag	p(mas)	Out	Days	SDSS	CRTS	Spec[a]	ID and Other Surveys[b]
18aabpwzq	16 22 07.16	+19 22 36.5	41.3	15.6–19.7	1.01 ± 0.17	3	317	Y	⋯	SD	V589 Her,G
18abaaewz	16 31 00.23	+69 50 01.2	37.2	17.2–21.0	⋯	HL	379	⋯	Y2	AP	AT2018fmi,ROSAT,XMM,G
18aaovjvr	16 52 44.83	+33 39 25.5	38.3	18.1–20.1	⋯	8	411	Y	Y1	SD	G
18aaiytds	17 27 58.13	+38 00 22.5	32.0	14.6–20.9	1.77 ± 0.14	4	389	Y	⋯	MDM	MOT,G
18aajtkma	17 30 08.36	+62 47 54.3	33.2	15.6–20.0	⋯	3	236	Y	⋯	SD	2MASS,G
18aalafea	17 31 02.22	+34 26 33.1	30.7	16.3–20.7	⋯	SOB	408	Y	Y1	AP	ASASSN-15 cm,G
18aakzxki	17 42 09.17	+23 48 29.4	25.2	14.2–20.0	1.26 ± 0.16	5	380	Y	Y3	⋯	V660 Her,AT2018cyb,G
18abetddh	17 47 14.33	+15 00 47.5	20.8	17.1–20.0	⋯	8	354	Y	Y2	⋯	G
18aajrvst	17 48 16.33	+50 17 22.9	30.4	16.4–20.6	⋯	11	386	Y	Y3	⋯	AT2016bnf,MOT,G
18aaslagi	18 05 46.35	+31 40 17.7	22.9	14.1–20.7	1.83 ± 0.18	2	365	⋯	Y4	⋯	V1008 Her,AT2019akt,G
18abbprmq	18 08 44.69	+34 27 23.9	23.2	17.8–20.0	⋯	SOB,1	101	⋯	⋯	⋯	V631 Her
18aamigoo	18 16 13.17	+49 52 05.1	25.9	12.3–15.5	11.40 ± 0.02	H,L	379	⋯	Y2	⋯	AM Her,G
18abdhozj	18 32 11.38	+61 55 06.0	25.9	15.8–19.0	⋯	2	339	⋯	⋯	AP	ASASSN-13ah,ATel5052,G
18aakzfjo	18 44 26.67	+37 59 51.9	17.6	13.5–20.0	2.22 ± 0.13	12	382	⋯	⋯	⋯	AY Lyr,AT2019njr,G
18aakzafr	18 44 39.18	+43 22 28.0	19.4	15.5–20.0	0.94 ± 0.08	5	379	⋯	Y2	⋯	V344 Lyr,G
18aapgtye	18 53 00.76	+45 27 08.2	18.7	16.0–20.0	0.86 ± 0.19	5	376	⋯	Y2	⋯	KIC,G
18abdkpgs	19 14 43.53	+60 52 13.8	20.8	15.3–19.9	⋯	1	336	⋯	⋯	⋯	CBET1535,AT2017eqn,K
18aavetqn	19 18 42.00	+44 49 12.4	14.3	15.5–21.0	1.22 ± 0.31	2	228	⋯	⋯	⋯	KIC,Gx,ATel6187,AT2018fao,G
18aaptcay	19 19 05.19	+48 15 06.1	15.6	18.5–22.7	⋯	9	378	⋯	⋯	⋯	AM CVn type,PTF1,G
18abcccnr	19 22 41.96	+52 43 59.0	16.8	14.0–21.0	⋯	4	327	⋯	⋯	⋯	V1113 Cyg,G
18aauefbw	19 27 48.53	+44 47 24.6	12.8	16.8–20.0	1.16 ± 0.17	2	371	⋯	⋯	⋯	KIC,G
18aaptcqq	19 44 19.29	+49 12 57.3	12.3	18.2–20.0	⋯	13	366	⋯	⋯	⋯	KIC, Gx
18abmszln	19 48 14.46	+34 52 01.1	4.7	16.4–20.8	⋯	2	277	⋯	⋯	⋯	V1153 Cyg,G
18aasncio	19 48 23.31	+36 26 23.0	5.4	14.0–20.0	1.95 ± 0.05	9	361	⋯	⋯	⋯	V811 Cyg,G
18aawbluo	19 53 04.93	+21 14 48.8	−3.2	15.5–19.2	0.62 ± 0.05	4	349	⋯	⋯	⋯	V405 Vul,G
18abobptn	19 57 18.83	−09 19 21.5	−18.8	12.6–18.6	3.19 ± 0.06	4	300	Y	Y2	⋯	UU Aql,G
18abjhdua	19 58 37.08	+16 41 28.4	−6.6	14.9–20.6	1.50 ± 0.34	1	76	⋯	⋯	⋯	AW Sge,G
18aawvwks	19 59 52.40	+39 13 59.8	4.9	15.3–20.7	⋯	2	347	⋯	⋯	⋯	V337 Cyg,G
18aavzjuw	20 00 05.22	+22 56 06.0	−3.7	17.0–20.0	0.76 ± 0.11	5	350	⋯	⋯	⋯	SW Vul,G
17aabopqx	20 12 13.66	+42 45 50.9	4.8	16.3–19.7	1.51 ± 0.14	4	342	⋯	⋯	⋯	V1316 Cyg,G
18aaypnnd	21 08 33.97	+39 05 35.3	−5.8	15.7–18.4	1.73 ± 0.07	6	332	⋯	⋯	⋯	Lanning386,G
18aazsdnv	21 26 24.12	+25 38 26.7	−17.7	14.3–20.8	1.88 ± 0.33	5	327	Y	⋯	⋯	MOT,AT2016gwu,ATel5111,K,G
17aaaqgbm	21 34 15.86	+49 11 26.3	−2.0	15.3–20.2	1.83 ± 0.12	1	331	⋯	⋯	⋯	V1081 Cyg,G
17aaawglf	21 44 03.78	+44 39 01.7	−6.5	15.7–20.0	0.99 ± 0.29	10	328	⋯	⋯	⋯	V2209 Cyg,G
18abcsuit	21 47 38.41	+24 45 54.0	−21.8	13.2–21.0	2.01 ± 0.22	3	208	Y	Y3	⋯	KIC,G
18abqdtes	21 54 33.97	+23 54 00.1	−23.5	16.2–21.0	⋯	2	106	⋯	⋯	SM	MOT,G
17aaaedpn	21 57 16.44	+52 12 00.8	−2.0	16.4–21.0	⋯	7	333	⋯	⋯	⋯	V1404 Cyg,G
18abcqadc	22 19 10.14	+31 35 22.8	−21.0	17.2–20.4	⋯	4	136	Y	Y2	⋯	PTF1,G
18abigrzf	22 21 44.77	+18 40 07.9	−31.6	13.3–19.0	5.23 ± 0.09	3	317	Y	Y1	SD	V521 Peg
18aaznfkp	22 23 04.66	+52 40 58.2	−3.9	15.7–20.0	⋯	3	328	⋯	⋯	⋯	MN Lac,G
18abtffxi	22 24 43.46	+50 31 39.1	−5.8	16.1–20.9	⋯	SOB	41	⋯	⋯	⋯	MR Lac
18abccqjx	22 43 40.73	+30 55 20.0	−24.4	13.7–17.1	1.36 ± 0.04	6	320	Y	Y3	⋯	V537 Peg,G

Notes.
[a] AP = APO DIS; K = Keck LRIS; P = Pal200in DBS; SD = SDSS; SM = SEDM; SP = SPRAT.
[b] MOT = MASTEROT; G = Gaia; Gx = GALEX; KIC = Kepler; K = Kato SH papers.

(This table is available in machine-readable form.)

Table 2
CV Candidates

ZTF	R.A.	Decl.	b°	Δmag	p(mas)	Out	Days	SDSS	CRTS	Spec[a]	Other Surveys[b]
18ablvaya	00 14 36.26	+50 32 39.9	−11.9	16.7–21.0	⋯	SOB,2	147	⋯	⋯	⋯	MOT,Gx,ATel5749,G
18abcrbtv	00 14 00.93	+59 48 02.8	−2.7	18.0–20.0	⋯	3	237	⋯	⋯	⋯	G
18abuocxn	00 17 09.52	+48 53 49.6	−13.6	15.1–21.0	⋯	SOB	92	⋯	⋯	⋯	G
18abgjgyt	00 20 09.52	+51 19 13.0	−11.2	17.6–20.6	⋯	4	235	⋯	⋯	⋯	G
18abgrzbs	00 33 03.96	+38 01 05.3	−24.7	16.0–20.8	1.48 ± 0.19	3	226	Y	Y7	⋯	AT2016dtx,G
17aabumcd	00 34 17.70	+43 45 39.3	−19.0	17.4–21.0	⋯	SOB	154	⋯	⋯	⋯	G
18aczower	00 34 59.91	+27 36 19.0	−35.1	18.3–20.4	⋯	3	264	Y	Y2	SDe	G
18accbuhi	00 36 15.24	+38 51 31.8	−23.9	18.5–23.0	⋯	SOB	36	Y	Y2	SP	PTF
18abmntno	00 47 30.31	+58 32 01.8	−4.3	16.0–20.0	⋯	2	182	⋯	⋯	⋯	G
17aaaeefu	00 59 43.51	+64 54 42.2	2.1	16.3–18.7	1.32 ± 0.07	6	250	⋯	⋯	⋯	G
18abgtrkj	01 12 37.73	+61 27 35.4	−1.3	16.2–20.1	1.10 ± 0.19	SOB	200	⋯	⋯	⋯	G
18abvytad	01 14 17.73	+59 35 54.7	−3.1	17.3–21.0	⋯	SOB	41	⋯	⋯	⋯	⋯
18abumrmx	01 15 16.55	+24 55 30.1	−37.6	16.6–19.5	⋯	2	300	Y	Y3	SDe	G
18abflqfh	01 17 12.39	+58 28 04.3	−4.2	16.5–19.6	⋯	8	234	⋯	⋯	⋯	G
17aaaruaj	01 28 36.51	+53 28 29.3	−9.0	18.0–21.0	⋯	7	233	⋯	⋯	⋯	MOT,Gx,ATel5395,G
18abzbknn	01 32 37.26	+60 36 09.3	−1.9	18.0–21.0	⋯	2	152	⋯	⋯	⋯	⋯
18abqasii	01 34 38.24	+52 06 15.9	−10.2	16.1–20.5	⋯	3	185	Y	⋯	⋯	G
18aabfagc	02 02 31.50	+56 23 38.9	−5.1	16.2–20.0	0.69 ± 0.14	8	228	⋯	⋯	⋯	G
18abtlqub	02 04 58.23	+57 28 06.9	−4.0	17.6–20.0	⋯	SOB	54	⋯	⋯	⋯	⋯
17aaatlsc	02 14 12.97	+52 25 56.8	−8.4	18.3–20.7	⋯	6	341	⋯	⋯	⋯	⋯
18aabfbek	02 45 07.91	+46 33 00.0	−12.0	16.1–19.9	⋯	2	37	Y	⋯	⋯	G
18ablwmaq	02 45 43.60	+63 16 48.7	3.2	17.3–20.1	⋯	3	224	⋯	⋯	⋯	G
18abtmqvh	03 32 24.87	+53 36 17.3	−2.1	16.5–20.0	⋯	2	207	⋯	⋯	⋯	G
18acsjgoa	03 42 46.18	+33 42 43.2	−16.8	17.7–20.5	⋯	2	122	⋯	Y3	⋯	G
18adarypz	04 01 17.42	+28 39 41.7	−18.0	16.9–20.5	⋯	SOB	45	⋯	Y1	⋯	⋯
18acuwgij	04 02 14.23	+22 08 35.5	−22.5	17.5–21.0	⋯	1	30	⋯	Y2	Pe	AT2018jrm
19aactcry	04 03 41.03	+47 56 26.4	−3.4	18.7–20.2	⋯	SOB	47	⋯	⋯	⋯	⋯
18aabffpk	04 22 15.21	+29 47 58.5	−14.0	17.7–20.2	⋯	6	171	Y	Y3	APe	G
18aaadvfu	04 28 37.10	+31 57 57.7	−11.5	17.5–20.8	⋯	5	131	⋯	Y2	⋯	G
18achqmhh	04 29 47.30	+18 47 48.4	−20.0	17.9–20.1	⋯	SOB	55	⋯	⋯	APe	AT2018ild
18acsjdxo	04 39 16.69	+15 26 33.6	−20.3	18.3–19.6	⋯	1	29	⋯	Y2	SPe	AT2018jkg
17aactzul	04 51 22.36	+16 10 19.5	−17.5	18.8–20.8	⋯	1	11	⋯	⋯	Ke	G
18aaadvfh	04 55 27.72	+38 58 59.0	−2.8	18.0–20.5	⋯	3	157	⋯	⋯	⋯	⋯
18abvlkyj	04 56 44.78	+50 45 32.8	4.8	18.0–21.0	⋯	SOB	42	⋯	⋯	⋯	⋯
17aaabekg	05 04 28.06	+44 46 37.5	2.1	17.6–20.2	⋯	4	251	⋯	⋯	⋯	G
18abuafzd	05 21 55.88	+38 52 15.1	1.3	16.0–21.0	⋯	1	85	⋯	⋯	⋯	G
17aaatnzw	05 24 04.33	+37 04 06.2	0.6	16.2–20.3	⋯	3	227	⋯	⋯	⋯	G
18abvtosb	05 28 55.68	+36 18 38.8	1.0	15.9–20.9	⋯	1	222	⋯	⋯	⋯	CBET,G
17aabdvhz	05 37 31.70	+50 15 21.4	9.8	17.5–19.0	⋯	4	226	⋯	⋯	⋯	G
17aaczwtq	05 53 33.12	+24 42 33.0	−0.7	17.3–20.7	⋯	2	97	⋯	⋯	⋯	G
18abuqngq	06 11 25.06	+22 21 17.1	1.7	16.8–20.0	⋯	2	229	⋯	⋯	⋯	PTF
17aaatdec	06 13 32.17	+06 57 07.6	−5.2	17.2–20.6	⋯	7	201	Y	⋯	⋯	G
18abyyhsf	06 16 00.22	+21 22 29.9	2.2	18.1–20.0	⋯	1	31	⋯	⋯	⋯	⋯
17aadbpoq	06 18 09.21	+27 38 24.4	5.6	15.6–20.0	⋯	SOB,3	411	⋯	⋯	⋯	G
17aacpcfj	06 19 52.22	+24 20 58.6	4.4	15.1–18.9	⋯	1	71	Y	⋯	⋯	G
18aaaanuc	06 21 23.26	+19 13 00.3	2.3	16.5–19.8	⋯	3	217	⋯	⋯	⋯	G
18aabtvzf	06 26 22.62	+19 46 32.6	3.6	16.6–20.6	⋯	3	469	⋯	⋯	⋯	G
17aabyrom	06 29 54.23	+25 39 11.8	7.0	16.2–20.9	⋯	3	336	Y	⋯	⋯	MOT,ATel6027,G

Table 2
(Continued)

ZTF	R.A.	Decl.	$b°$	Δmag	p(mas)	Out	Days	SDSS	CRTS	Spec[a]	Other Surveys[b]
17aacmlmj	06 31 27.16	+22 12 26.7	5.8	17.6–20.6	⋯	SOB	39	⋯	⋯	⋯	⋯
18abypyap	06 31 45.99	+09 54 45.2	0.2	16.8–20.1	⋯	2	109	Y	⋯	⋯	⋯
18abztcib	06 33 30.75	+59 18 47.8	20.9	15.5–20.8	⋯	2	218	⋯	⋯	SM	AT2018gxm
19aakmorl	06 37 33.01	−09 35 42.1	−7.4	11.3–19.3	2.72 ± 0.44	1	79	⋯	⋯	⋯	AT2019dhk,G
18achtpcj	06 41 21.30	+44 41 05.6	17.0	17.3–20.2	⋯	SOB	36	Y	⋯	⋯	AT2018ila
17aaaoxxi	06 49 01.96	+08 59 44.6	3.6	16.6–20.1	⋯	5	449	⋯	⋯	⋯	G
17aabziqr	06 52 13.34	+30 57 22.2	13.7	15.7–21.0	⋯	6	545	⋯	⋯	⋯	G
19aaekpin	06 54 04.39	−09 41 03.5	−3.8	16.3–20.5	⋯	SOB	59	⋯	⋯	⋯	AT2019awv,ROSAT
18acphaci	06 55 50.84	−09 32 37.6	−3.4	17.5–20.6	⋯	6	150	⋯	⋯	⋯	G
18acuxkzq	07 04 37.59	+06 01 13.3	5.7	17.6–20.0	⋯	SOB	36	⋯	⋯	⋯	AT2018jii
18acpvmnu	07 07 35.97	−09 12 41.7	−0.6	15.0–20.5	⋯	2	67	⋯	⋯	⋯	AT2018itx,G
18acnnxrd	07 11 28.27	−03 26 15.0	2.9	16.5–20.0	⋯	SOB,1	117	⋯	⋯	SM	G
18acuxvld	07 15 12.98	−06 42 38.3	2.2	14.6–19.0	⋯	SOB	31	⋯	⋯	⋯	G
18acvvthl	07 49 40.33	+07 15 56.0	16.2	17.3–19.9	⋯	1	16	Y	⋯	⋯	MOT
18acqxeba	08 03 16.61	+66 11 10.0	31.9	15.0–17.9	0.87 ± 0.25	1	153	Y	⋯	⋯	G
18aabuaxp	08 19 31.24	+21 33 38.0	28.5	17.4–20.2	⋯	3	508	Y	Y6	SMe	G
18aabjjuj	09 11 47.01	+31 51 01.8	42.5	14.8–20.5	⋯	SOB,1	134	Y	Y4	⋯	G
18acnocdo	09 14 42.69	+67 10 36.9	38.5	15.0–20.1	1.12 ± 0.33	SOB	181	Y		APe	G
18aczejci	09 26 20.42	+03 45 42.4	35.8	17.6–20.5	⋯	6	144	Y	Y2	⋯	G
18aabywzu	10 37 38.65	+12 42 50.1	55.6	16.6–20.3	⋯	1	84	⋯	Y2	SMe	AT2016ags
17aaclmhw	10 53 33.76	+28 50 35.7	64.0	17.9–19.9	⋯	3	111	Y	⋯	K,We	⋯
19aacyjjz	11 10 18.95	−05 22 18.4	49.3	16.4–20.0	⋯	1	171	⋯	Y2	⋯	ATel1272,G
18aaqepuc	11 37 08.67	+51 34 50.9	61.8	17.4–20.8	⋯	3	375	Y	Y4	⋯	G
18abbghiz	12 56 09.84	+62 37 04.4	54.5	16.5–21.5	⋯	SOB	43	Y	⋯	⋯	MOT,ATel8846
18aabqewr	12 58 32.22	+26 01 06.0	88.1	16.0–21.0	1.14 ± 0.05	1	511	Y	⋯	⋯	ASASSN-18cr
18aabxycb	13 15 14.42	+42 47 44.6	73.6	16.9–20.5	⋯	9	511	Y	Y8	APe,We	PTF,G
18aajlfdq	13 56 42.38	+61 30 24.4	53.9	16.4–21.4	⋯	2	387	Y	⋯	⋯	ASASSN-13ap,ATel5118,G
18aawqkva	15 44 28.10	+33 57 26.4	52.4	17.1–24.0	⋯	3	410	Y	Y2	⋯	AT2018fhi,PTF
18aavojbe	15 46 52.71	+37 54 14.9	51.9	16.0–21.1	⋯	2	350	Y	Y4	⋯	PTF,G
18abklaip	15 50 30.38	−00 14 17.4	39.0	18.1–19.5	⋯	2	275	Y	Y2	⋯	G
18aakuohk	16 17 00.94	+62 00 24.6	41.6	14.7–20.5	2.03 ± 0.08	10	384	Y	Y2	⋯	PTF,G
18abagclj	16 26 05.66	+22 50 43.5	41.5	18.3–20.6	⋯	SOB,1	356	Y	Y3	⋯	CRTS
18aakvnlw	16 47 48.00	+43 38 45.0	40.2	19.4–20.4	⋯	7	174	⋯	Y1	We	G
18abkikam	17 04 44.51	+26 20 28.5	34.1	19.5–20.7	⋯	1	31	Y	⋯	SM,Ke	⋯
18aaisdps	17 05 15.33	+72 44 03.2	33.6	16.5–20.8	⋯	6	309	Y	⋯	⋯	MOT,G
18abpaake	17 06 06.10	+25 51 53.2	33.7	16.4–20.3	⋯	1	32	Y	⋯	⋯	⋯
19aagdvdi	17 11 38.40	+05 39 50.9	24.7	15.2–20.1	⋯	2	106	⋯	⋯	⋯	PTF,AT2019ath,G
18abeechv	17 16 02.90	+29 27 36.5	32.5	18.8–20.0	⋯	SOB	45	Y	⋯	Pe	⋯
18abfwukx	17 26 24.11	+36 25 06.3	32.0	19.2–21.0	⋯	1	37	⋯	⋯	Ke	AT2018eky
19aanvbqa	17 27 50.17	+23 52 47.5	28.4	14.8–20.0	⋯	SOB	64	Y	⋯	⋯	AT2019cni
18aapqotx	17 32 30.30	+50 09 32.6	32.9	17.5–20.0	⋯	2SOB	385	⋯	Y2	⋯	PTF,G
18aakzqjh	17 46 48.85	+19 47 44.5	22.8	18.0–21.0	⋯	10	360	Y	Y2	⋯	G
18aaploaw	17 47 25.61	+63 02 47.9	31.2	18.0–20.4	⋯	3	409	Y	⋯	⋯	AT2018eeb,ATLAS18spw
18aajrtmo	17 48 27.86	+50 50 39.7	30.4	14.9–20.5	1.35 ± 0.25	5	408	Y	Y1	⋯	ASASSN-13ak,PTF,G
18abckxfb	17 49 21.78	+19 44 22.9	22.2	18.4–21.0	⋯	SOB	47	⋯	⋯	SM	AT2016cya
18abffzyg	17 52 38.47	+07 33 04.5	16.5	15.8–20.5	⋯	4	261	⋯	⋯	⋯	V982 Oph,G
18abfmuvj	17 53 30.49	+20 38 07.1	21.7	17.8–21.0	⋯	2	329	⋯	⋯	SM	AT2018dyr

Table 2
(Continued)

ZTF	R.A.	Decl.	b°	Δmag	p(mas)	Out	Days	SDSS	CRTS	Spec[a]	Other Surveys[b]
18aasfpxf	17 56 33.39	+57 29 26.6	29.9	17.5–21.0	⋯	2	384	Y	⋯	⋯	G
18aabtvdf	17 56 39.55	+44 40 12.4	28.1	15.3–21.0	0.72 ± 0.06	22	426	⋯	⋯	⋯	G
18aaumvgk	18 00 18.30	+15 15 28.4	18.1	16.5–20.0	⋯	1	279	⋯	⋯	SM,APe	MOT,AT2018bsp,ATEL9204
18aapauoa	18 00 43.08	+21 01 34.2	20.2	17.0–20.6	⋯	6	382	⋯	⋯	⋯	G
18aagrotg	18 02 31.35	+30 58 29.1	23.2	16.6–21.0	⋯	5	388	⋯	⋯	⋯	G
18abcmsux	18 03 24.75	+17 52 31.6	18.4	18.2–21.0	⋯	2SOB,1	315	⋯	⋯	⋯	AT2018fpf
18aayzgkc	18 10 20.69	+32 39 13.8	22.3	16.4–22.0	⋯	SOB	73	⋯	⋯	SM,APe	⋯
18abjvmhv	18 15 27.34	+41 56 05.3	24.1	13.8–21.0	⋯	SOB	299	Y	⋯	⋯	G
18aaptdcp	18 21 22.52	+61 48 55.2	27.2	14.3–21.1	1.15 ± 0.29	3	373	⋯	⋯	⋯	ASASSN-13at,G
18aaqznkg	18 29 13.38	+31 06 23.6	18.0	19.5–21.8	⋯	1	9	⋯	⋯	SM,Ke	MOT, AT2018bhx
19aaedxnl	18 30 07.21	+76 43 13.8	27.6	16.2–20.5	⋯	2	114	⋯	⋯	⋯	MOT,ATel4843,G
18aakytes	18 31 20.68	+30 19 34.9	17.3	16.1–21.0	⋯	5	390	⋯	⋯	⋯	MOT,ATel4761
18acaqbgu	18 34 35.96	+31 32 00.9	17.1	17.6–21.0	⋯	1	30	⋯	⋯	⋯	AT2016hrt,XMM,ROSAT
18abfgyjt	18 34 59.52	+54 33 15.0	24.1	17.9–21.0	⋯	2	31	⋯	⋯	Pe	⋯
18abdklug	18 37 05.92	+37 17 58.8	18.7	18.5–20.0	⋯	2	336	⋯	⋯	⋯	AT2018haz
18aatzhmn	18 41 51.05	+37 52 28.6	18.0	14.3–20.0	⋯	SOB	78	⋯	⋯	⋯	AT2018blk,G
18aaracvu	18 41 59.71	+37 34 11.6	17.9	17.8–20.0	⋯	SOB,6	106	⋯	⋯	K,APe	AT2018bit
18acdwdgx	18 42 51.29	+33 56 49.5	16.4	16.8–19.8	⋯	1	30	⋯	⋯	⋯	G
18aammzjo	18 44 26.89	+36 51 40.2	17.2	17.8–20.6	⋯	12	410	⋯	⋯	⋯	MOT,ATel6003,G
18aavyoqk	18 45 03.01	+13 55 17.6	7.7	14.9–18.9	⋯	6	350	⋯	⋯	⋯	ROSAT,G
18abfxhyn	18 46 12.88	+12 52 29.0	7.0	17.2–20.8	⋯	SOB	328	⋯	⋯	⋯	MOT
18ablrvfh	18 47 15.37	−06 13 21.0	−1.9	16.8–19.6	⋯	4	273	⋯	⋯	⋯	ROSAT,G
18abcysbr	18 48 43.45	+29 54 51.1	13.7	16.4–19.0	⋯	SOB,2	279	⋯	⋯	⋯	MOT
18abixdpa	18 50 22.30	+74 56 02.5	26.2	17.1–20.4	⋯	3	304	⋯	⋯	⋯	⋯
18aawadah	18 52 16.40	+15 06 23.5	2.1	16.4–20.5	⋯	3	377	⋯	⋯	⋯	G
18abbtilo	18 57 44.62	+32 13 46.5	12.9	18.3–21.0	⋯	SOB	38	⋯	⋯	APe	PTF
18aaovfjr	18 58 11.15	+46 27 56.5	18.2	15.4–20.4	1.42 ± 0.28	6	376	⋯	Y1	⋯	AT2017dac,G
18abqazwf	19 00 32.27	+30 30 40.0	11.6	17.9–20.0	⋯	2	270	⋯	⋯	Pe	⋯
18aaraifg	19 00 58.43	+30 35 47.5	11.6	17.6–21.0	⋯	SOB,1	33	⋯	⋯	SM,Pe	AT2018bhy
18accntcd	19 01 04.62	+45 05 16.0	17.2	17.1–21.0	⋯	SOB,1	201	⋯	⋯	⋯	AT2018ijr
18aapuklg	19 03 42.18	+53 47 45.8	19.8	15.3–21.0	0.99 ± 0.15	SOB,11	378	⋯	Y6	⋯	G
18abjkhgu	19 05 16.00	+47 23 34.5	17.4	17.1–20.7	⋯	SOB	288	⋯	⋯	⋯	MOT,Atel9104
18abciqza	19 08 12.64	+04 57 28.0	−1.5	17.3–20.1	0.88 ± 0.14	3	319	⋯	⋯	⋯	G
18abcyzxp	19 08 59.31	+25 39 45.7	7.8	17.6–19.1	⋯	1	10	⋯	⋯	⋯	G
18aavesgh	19 14 04.90	+47 25 10.0	16.0	16.1–20.7	⋯	2	374	⋯	⋯	⋯	G
18aayupbw	19 20 30.90	+27 43 33.1	6.5	17.4–21.0	⋯	1	280	⋯	⋯	⋯	G
18aapsxwc	19 20 58.71	+45 06 37.6	14.0	18.2–20.0	⋯	6	373	⋯	⋯	⋯	⋯
18aasnlwa	19 22 34.05	+27 32 01.1	6.0	16.5–20.9	⋯	7	371	⋯	⋯	⋯	G
18abkhgfg	19 26 33.86	+16 02 20.3	−0.3	16.9–20.3	⋯	SOB	42	Y	⋯	⋯	AT2016hkw
18aayncoh	19 27 57.59	+46 43 32.3	13.6	17.6–20.8	⋯	4	367	⋯	⋯	⋯	⋯
18abdeelv	19 30 59.19	+51 57 35.2	15.4	14.8–22.0	⋯	SOB	327	⋯	⋯	⋯	ASASSN-14fu,ATel6761,G
18aauegwi	19 32 03.61	+45 07 59.2	12.3	16.0–20.0	1.14 ± 0.14	5	373	⋯	⋯	⋯	G
18abptyvl	19 35 57.46	+11 05 28.2	−4.6	15.6–20.8	1.38 ± 0.43	2	282	⋯	⋯	⋯	G
18abdkwtr	19 35 57.54	+33 00 49.4	6.0	18.4–20.0	⋯	3	322	⋯	⋯	⋯	⋯
18abbctvx	19 36 02.88	+46 08 31.2	12.1	17.1–20.0	⋯	1	31	⋯	⋯	SM	⋯
18abdiirq	19 41 04.86	+31 57 47.7	4.5	15.4–21.0	0.71 ± 0.06	8	309	⋯	⋯	⋯	G
18aaynycd	19 42 30.55	+36 01 19.3	6.3	18.3–20.1	⋯	SOB	39	Y	⋯	SM	⋯

Table 2
(Continued)

ZTF	R.A.	Decl.	$b°$	Δmag	p(mas)	Out	Days	SDSS	CRTS	Spec[a]	Other Surveys[b]
18aazvbyj	19 43 32.98	+16 31 06.8	−3.6	17.5–19.5	⋯	5	319	⋯	⋯	⋯	G
18abdkpol	19 43 41.51	+43 59 11.9	9.7	18.2–20.5	⋯	2	114	⋯	⋯	⋯	⋯
18aaptabw	19 47 30.06	+48 09 17.6	11.3	16.1–21.2	⋯	3	358	⋯	⋯	⋯	PTF
18abfhssx	19 48 26.68	+59 33 10.3	16.4	19.0–21.0	⋯	2	145	⋯	⋯	SM	
18aauebur	19 48 49.10	+46 30 36.1	10.3	18.5–21.0	⋯	SOB,4	193	⋯	⋯	SM	AT2018epr
18ablxhlc	19 48 58.30	+58 26 20.9	15.8	18.2–21.0	⋯	SOB	300	⋯	⋯	⋯	G
18abmfxml	19 50 42.77	+08 25 45.3	−9.1	16.8–19.7	⋯	6	265	⋯	⋯	⋯	G
18abchfow	19 50 38.85	+21 16 51.8	−2.7	18.6–21.0	⋯	3	349	⋯	⋯	⋯	⋯
18aavzkpp	19 50 54.38	+35 51 35.9	4.7	17.7–21.0	⋯	3	211	Y	⋯	⋯	AT2019bcl,G
18aazfbvg	19 54 46.08	+18 37 57.3	−4.8	16.2–17.6	⋯	8	330	⋯	⋯	APe	PTF,G
18aaypfws	19 55 37.25	+23 35 57.9	−2.5	19.0–21.0	⋯	4	349	⋯	⋯	⋯	G
18aayecz t	19 57 12.21	+18 49 41.0	−5.2	16.5–19.0	⋯	2	174	⋯	⋯	⋯	G
18abvokyy	19 57 15.07	+36 27 03.3	3.9	18.0–21.0	⋯	2	89	⋯	⋯	⋯	G
18aawlljc	20 03 34.02	+29 34 36.7	−0.8	17.4–20.7	⋯	2	369	⋯	⋯	SM	AT2018ccf,G
18abmhjpr	20 04 07.64	+12 26 18.4	−10.0	16.4–19.5	0.99 ± 0.22	5	272	Y	⋯	⋯	G
18abnudvw	20 04 20.95	+11 32 47.2	−10.5	18.5–20.0	⋯	4	268	Y	⋯	⋯	AT2016diu,G
18acyjvhm	20 06 16.59	+07 38 15.4	−12.8	15.9–19.8	⋯	SOB	18	⋯	⋯	⋯	⋯
18absihoy	20 07 42.61	+11 58 10.4	−10.9	16.5–20.0	⋯	2	140	⋯	⋯	⋯	⋯
18abudsie	20 07 44.61	−00 27 50.1	−16.7	18.1–19.8	⋯	3	266	Y	⋯	⋯	G
18abaqnny	20 09 22.90	+59 13 48.1	13.9	19.2–24.0	⋯	2	70	Y	⋯	K	⋯
18aayukga	20 10 02.01	+37 06 15.4	2.1	17.5–20.8	⋯	6	329	⋯	⋯	⋯	G
18aaxyrau	20 10 53.41	+44 10 46.3	5.8	17.4–19.7	⋯	SOB,5	338	⋯	⋯	⋯	MOT,ATel4611
18aawluad	20 12 25.84	+23 36 20.9	−5.7	18.5–21.0	⋯	3	348	⋯	⋯	⋯	G
18abnuekr	20 13 55.88	−05 26 06.1	−20.8	17.2–19.5	⋯	3	259	⋯	⋯	⋯	G
18aayeosh	20 26 23.46	+32 01 08.4	−3.6	15.7–21.0	⋯	5	346	⋯	⋯	⋯	G
18aazffjy	20 28 36.83	+56 13 46.3	10.1	18.2–21.0	⋯	SOB,4	342	⋯	⋯	SM	⋯
18abajlni	20 32 32.12	+58 09 28.8	10.8	16.7–21.0	⋯	SOB,2	286	Y	⋯	SM	⋯
18abssrbs	20 35 01.48	−00 19 46.4	−23.0	15.6–20.0	1.17 ± 0.25	1	263	Y	Y3	⋯	ASASSN-14hb,AT2019gya,G
18aaxprrt	20 36 39.95	+47 02 15.8	3.7	17.8–21.0	⋯	3	316	⋯	⋯	⋯	G
18acbwqtc	20 40 44.21	+50 59 40.2	5.6	16.0–21.0	⋯	SOB	39	⋯	⋯	⋯	⋯
18abikzev	20 41 30.41	+48 13 33.0	3.8	18.6–20.5	⋯	3	319	⋯	⋯	⋯	G
18abdhxvl	20 43 59.58	+42 03 25.4	−0.4	16.8–19.5	1.49 ± 0.45	6	335	Y	⋯	⋯	AT2016dvk,G
18abxkbzz	20 44 28.70	+14 50 11.3	−16.9	18.4–21.0	⋯	SOB	39	Y	⋯	SM	AT2018grl
18abzvpif	20 49 51.90	+46 19 50.2	1.5	18.5–20.5	⋯	1	249	⋯	⋯	⋯	⋯
18abjwsby	20 59 15.71	+43 01 07.2	−1.9	17.4–20.0	0.45 ± 0.12	3	308	⋯	⋯	⋯	G
18aazeyze	21 04 35.46	+15 05 01.4	−20.7	18.0–20.3	⋯	4	329	⋯	⋯	⋯	G
18abmarba	21 21 08.93	+30 34 14.3	−13.5	16.0–20.8	⋯	2	287	⋯	⋯	⋯	G
17aaaejau	21 21 28.58	+29 15 41.2	−14.5	17.5–20.7	⋯	5	293	⋯	⋯	⋯	AT2018kgn,G
18absanfq	21 23 05.54	+15 08 48.6	−24.1	17.8–21.0	⋯	1	42	⋯	⋯	SM	AT2018fpd
18aayoxjs	21 25 43.95	+63 23 18.0	9.2	17.6–19.9	⋯	SOB,5	334	⋯	⋯	SM	AT2018efi,G
18abihypg	21 28 22.20	+63 25 57.2	9.0	15.0–20.0	⋯	6	320	⋯	⋯	We	G
18abvigco	21 29 59.49	+78 52 21.5	19.7	14.8–20.0	1.89 ± 0.32	SOB	45	⋯	⋯	⋯	G
18abwntpz	21 34 37.09	+57 02 07.3	3.8	14.9–20.6	⋯	SOB	220	⋯	⋯	⋯	G
18abaphmn	21 38 25.68	+27 30 36.0	−18.4	18.9–21.0	⋯	SOB	102	Y	⋯	⋯	AT2016fvd
18abjtach	21 43 32.98	+46 12 22.3	−5.2	16.7–20.5	⋯	SOB	33	⋯	⋯	⋯	G
17aadsnyp	21 43 33.57	+51 20 03.7	−1.3	16.9–20.9	0.52 ± 0.13	7	331	⋯	⋯	⋯	G
17aaarine	21 46 48.25	+48 27 47.5	−3.9	18.1–21.0	⋯	2 SOB	122	Y	⋯	⋯	AT2016jbf

Table 2
(Continued)

ZTF	R.A.	Decl.	$b°$	Δmag	p(mas)	Out	Days	SDSS	CRTS	Spec[a]	Other Surveys[b]
18abnxgmb	21 48 07.80	+29 38 48.0	−18.3	16.4–21.0	⋯	SOB	163	⋯	⋯	⋯	G
18abochac	21 51 25.83	+46 28 03.5	−5.9	18.2–22.0	⋯	2	174	Y	⋯	⋯	G
18abvxdou	21 52 32.31	+49 04 19.4	−4.0	16.7–21.0	⋯	SOB,1	263	⋯	⋯	⋯	AT2018glg
17aabutiy	21 58 15.94	+51 50 20.3	−2.4	17.4–19.8	⋯	3	336	⋯	⋯	⋯	G
18abvbqyo	22 06 41.05	+30 14 35.8	−20.4	18.4–21.0	⋯	2	234	Y	Y1	SM	AT2016jai
18acarunx	22 14 03.77	+37 34 52.8	−15.5	17.5–20.0	⋯	2	254	⋯	⋯	⋯	AT2018hgp
18abmnbne	22 17 31.66	+46 59 32.9	−8.2	17.3–20.4	⋯	SOB	67	⋯	⋯	⋯	⋯
18ablvntg	22 27 07.17	+55 38 00.0	−1.7	15.2–20.6	1.60 ± 0.39	1	41	⋯	⋯	SMe	G
18abqboud	22 31 23.00	+33 30 57.1	−20.6	15.5–21.0	⋯	SOB	108	⋯	⋯	SM	AT2018frz
18abblwnw	22 45 00.98	+56 31 30.6	−2.2	16.8–20.3	⋯	4	328	⋯	⋯	⋯	G
18actxlqb	22 45 05.38	+01 15 47.2	−48.4	18.4–21.6	⋯	1	28	Y	Y4	⋯	AT2018jlx
18abmnmuw	22 47 51.45	+36 43 19.3	−19.8	15.7–20.4	⋯	1	41	Y3	⋯	⋯	MOT,ATel7438,G
18acehgym	22 48 25.98	+38 55 09.6	−18.0	19.2–23.0	⋯	2	32	⋯	⋯	SM,Ke	AT2018hgz
18abccwds	22 52 31.58	+59 11 35.1	−0.2	18.9–21.0	⋯	4	364	⋯	⋯	⋯	G
18abmnmvz	22 53 50.55	+33 30 32.4	−23.3	16.2–20.2	⋯	3	159	Y	Y2	⋯	ASASSN-13by,G
18abvburn	22 55 21.40	+53 38 43.8	−5.4	18.7–20.9	⋯	1	40	⋯	⋯	⋯	⋯
18ablvjse	22 56 32.43	+35 42 38.4	−21.6	17.0–21.0	⋯	3	297	⋯	Y2	APe	MOT,G
18abcxmen	22 56 57.90	+55 53 41.6	−3.5	17.6–21.0	⋯	7	197	⋯	⋯	⋯	⋯
18aaypqid	23 05 38.42	+65 21 58.6	4.7	14.7–20.5	1.62 ± 0.23	1	332	⋯	⋯	⋯	ROSAT,G
18aazndjw	23 10 11.15	+51 15 11.1	−8.5	17.6–20.5	⋯	SOB	329	⋯	⋯	SM	ATel11797,AT2018ctl,ROSAT,G
18aazwddf	23 24 04.01	+51 43 18.0	−8.8	17.3–21.4	⋯	4	328	Y	⋯	⋯	⋯
17aabunmx	23 34 35.56	+54 33 25.5	−6.7	15.7–20.5	1.19 ± 0.19	SOB,3	225	⋯	⋯	⋯	AT2018asi,G
18abvxbfh	23 35 30.00	+60 54 05.7	−0.6	17.4–20.3	⋯	1	52	⋯	⋯	⋯	⋯
17aabuvei	23 36 46.10	+57 57 24.1	−3.5	17.7–20.0	⋯	7	231	⋯	⋯	⋯	G
18abcpbbj	23 37 27.57	+51 13 58.7	−10.0	16.7–21.0	1.71 ± 0.33	3	206	⋯	⋯	⋯	G
18abjmxql	23 38 43.54	+57 17 19.9	−4.2	15.2–20.4	⋯	2	143	Y	⋯	⋯	G
18abiwzlg	23 52 01.18	+44 50 58.2	−16.8	15.2–20.4	1.60 ± 0.26	SOB,1	178	⋯	Y1	⋯	AT2016,G
17aaaedem	23 54 58.63	+54 27 29.3	−7.5	17.0–21.0	⋯	SOB,5	205	⋯	⋯	⋯	⋯
18abgtjea	23 59 33.64	+56 05 01.5	−6.1	17.6–21.0	⋯	SOB	65	⋯	⋯	⋯	AT2018eoi,ATLAS

Notes.
[a] AP = APO DIS; K = Keck LRIS; P = Pal200in DBS; SD = SDSS; SM = SEDM; SP = SPRAT; W = WHT.
[b] MOT = MASTEROT; G = Gaia; Gx = GALEX.

(This table is available in machine-readable form.)

Table 3
Possible CV Candidates

ZTF	R.A.	Decl.	$b°$	Δmag	p(mas)	Out	Days	SDSS	CRTS	Spec	Surveys
18abhypsw	00 52 09.61	+43 56 20.1	−18.9	17.0–20.0	0.50 ± 0.07	2	49	Y	Y2	⋯	ROSAT,G
18acyqzew	01 43 54.23	+29 01 03.8	−32.5	15.8–19.0	⋯	1	42	Y	Y2	⋯	⋯
18abppgdj	03 28 15.91	+61 25 17.2	4.0	14.2–20.5	4.09 ± 0.15	1	219	⋯	⋯	⋯	AT2019cbz,G
17aaaaqee	04 43 17.84	+54 02 27.6	5.3	16.7–21.0	0.25 ± 0.04	1	14	⋯	⋯	⋯	⋯
18acemvzp	04 57 51.59	−06 10 38.2	−28.0	16.4–20.4	1.10 ± 0.05	1	14	⋯	⋯	⋯	ROSAT,G
17aaabswj	05 25 03.73	+39 33 59.1	2.2	17.6–19.6	1.69 ± 0.56	2	193	⋯	⋯	⋯	G
18adaifhl	05 35 45.89	−08 47 48.8	−20.8	18.6–20.0	⋯	1	30	⋯	⋯	⋯	AT2018lu,ROSAT
18acxhxny	05 47 04.15	+26 45 04.0	−0.9	17.2–21.0	⋯	1	29	⋯	⋯	⋯	⋯
18acnatft	06 29 04.48	+11 25 37.5	0.3	17.8–21.0	⋯	1	14	⋯	⋯	⋯	⋯
19aakncwr	08 10 51.92	−04 04 28.5	15.6	16.4–20.2	⋯	1	53	⋯	⋯	⋯	AT2017cjw
18acrhioo	08 40 19.19	−03 51 24.7	22.1	17.2–19.3	⋯	2	35	⋯	⋯	⋯	⋯
19aajywdx	09 24 34.29	+08 40 31	37.9	16.2–20.7	⋯	1	24	Y	⋯	⋯	⋯
19aarflna	11 34 02.27	+14 01 29.3	67.7	13.6–20.0	⋯	1	26	Y	⋯	⋯	⋯
19aaqxmmw	14 58 58.58	−06 07 05.8	44.7	15.4–20.3	⋯	1	23	⋯	⋯	⋯	⋯
18abetcrn	17 28 03.39	+25 50 50.3	28.9	19.4–21.1	⋯	2	296	⋯	⋯	P,K	⋯
18abltirl	18 06 56.21	+06 10 34.8	12.7	15.9–21.0	1.93 ± 0.19	2	341	⋯	⋯	⋯	Swift,G
18aaniudh	18 09 47.90	+30 23 05.7	21.7	16,9–19.5	0.84 ± 0.03	3	379	⋯	Y2	⋯	⋯
18ablmpfr	18 44 34.47	+13 07 17.7	7.4	19.0–21.0	⋯	1	30	⋯	⋯	⋯	G
18abdjqmg	19 38 44.34	+35 40 31.2	6.8	17.5–19.9	⋯	1	30	Y	⋯	⋯	⋯
19aaaaazu	20 27 03.59	+19 23 07.9	−10.9	15.4–19.4	⋯	SOB?	35	⋯	⋯	⋯	⋯
18accpmqr	20 55 08.85	−06 29 11.4	−30.4	17.0–19.6	⋯	2	48	Y	⋯	⋯	⋯

(This table is available in machine-readable form.)

Marshal light curves, the interval of actual coverage by ZTF in days up to 2019 May 8, if the source is in the Sloan Digital Sky Survey (SDSS) footprint, the number of outbursts visible in CRTS if covered by that survey, any spectra obtained with the ZTF instruments or available from the SDSS or the literature, and any other relevant information.

The easiest systems to classify as CVs are those that show a long string of observations at quiescence along with one SOB that has a large amplitude (typically 5–9 mag) and a long duration (typically 3 weeks). A typical example (ZTF1727+23) is shown in Figure 1. The SOB often has a distinct shape, with a linear, slowly declining plateau following the peak magnitude that lasts for 1–2 weeks, then a steep decrease toward the quiescent magnitude. In a few cases, there are one or more rebrightening episodes during the decline (examples are ZTF2231+33 with one rebrightening and ZTF184159+37 with six possible rebrightnenings shown in Figure 1). These systems are known as WZ Sge stars (Warner 1995) or Tremendous Outburst Amplitude Dwarf Novae (TOADS; Howell et al. 1995). Modeling of TOADS has shown that they are the systems with the lowest accretion rates among dwarf novae (Howell et al. 1995) and the ones that population synthesis models (Howell et al. 1997, 2001) predict should be the most numerous in surveys of CVs. They should have evolved to the shortest orbital periods in their evolution during the lifetime of the Galaxy. Most dwarf novae that have orbital periods less than 2 hr show both SOBs and normal outbursts. The systems with larger accretion rates are generally those with longer orbital periods and with short recurrence times for outbursts, so they are readily found in sky surveys with coverage of weeks to months. An example of this kind of system is ZTF0613+06 in Figure 1. All objects in Table 2 show outbursts with one of the types described above. There also exist NL systems which do not show outbursts but do exhibit high and low states of accretion that last for many days. Two of these previously known systems, ZTF0854+39 (FR Lyn) and ZTF1631+69 (shown in Figure 2), were found in the Marshal, but none of the candidates in Tables 2 or 3 showed this behavior. The filter works best to detect outburst behavior and will need to be modified to pick up the generally slower transitions between high and low states.

For the most part, the objects in Table 3 did not have enough data to unambiguously determine if their variability is due to a dwarf nova outburst or to some type of pulsational instability. As the survey proceeds, more observations may provide an unambiguous classification.

3.1. Spectroscopic Confirmations

Many of the SEDM spectra were obtained near outburst, when the accretion disk is dominant and producing a blue continuum or weak absorption lines. Thus, the low resolution usually only showed the continuum. The higher resolution and larger telescopes of the Palomar 200 in, Keck, WHT, and APO enabled better determination of Balmer and Helium emission lines as the systems evolved to quiescence. In addition, two candidates were found to have spectra available from SDSS. In total, 29 of the systems in Table 2 were able to be positively confirmed as CVs with noticeable Balmer or Helium emission lines (those designated with a small letter "e" in the Spec column of Table 2). Figure 3 shows the blue and red emission line spectra from the ZTF Marshal follow-up (coverage from 4000 to 9000 Å) while Figure 4 shows the red region from 5500 to 9000 Å) available from APO data when the blue side was not operational.

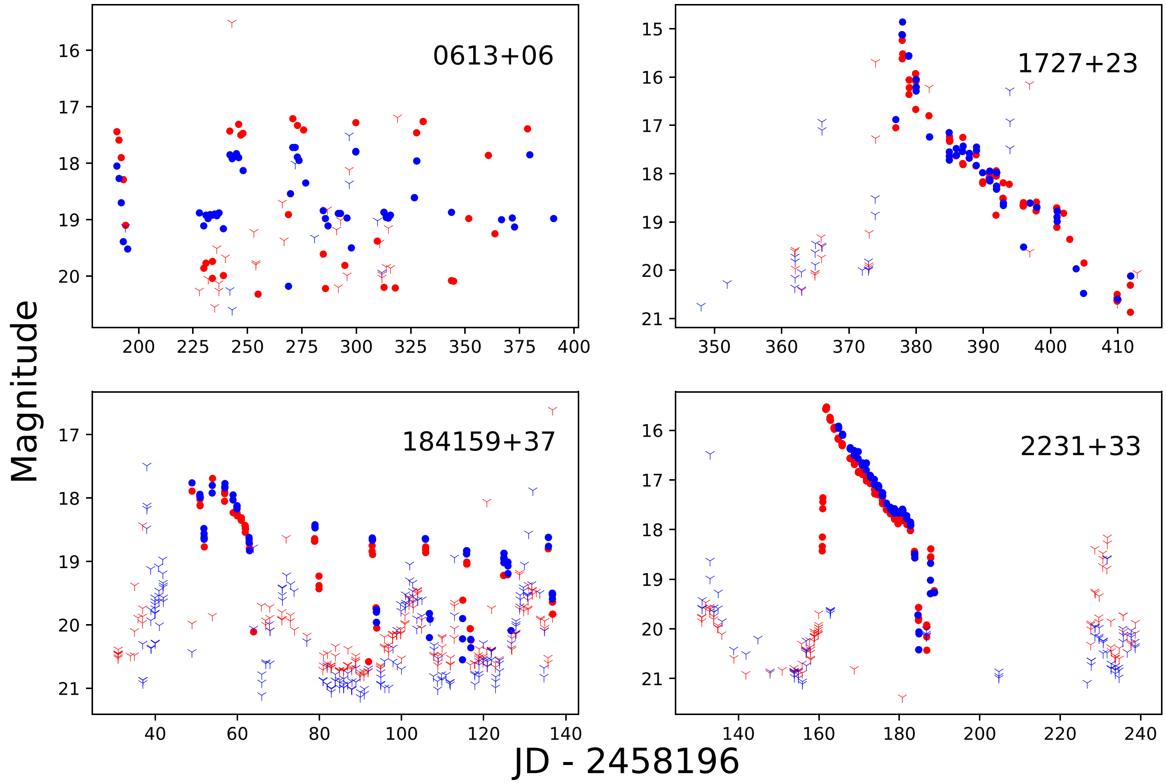

Figure 1. Examples of ZTF light curves of good CV candidates from Table 2. Filled blue and red circles are magnitudes from *g* and *r* filters, while light symbols are upper limits on those nights. ZTF1727+23 and ZTF2231+33 are examples of SOBs with an outburst lasting more than 20 days and a distinctive shape. They are likely WZ Sge type systems. ZTF184159+37 shows multiple rebrightenings after its SOB and is a candidate for an ER-UMa-type system. ZTF0613+06 shows repeated normal outbursts with low amplitude and is likely a typical dwarf nova with a relatively high-mass transfer rate.

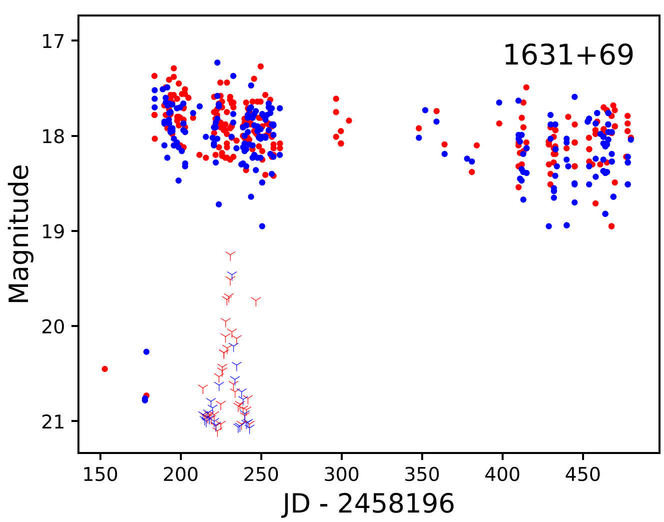

Figure 2. Example of a system showing high and low states. Symbols are the same as those in Figure 1.

3.2. The Galactic Plane

One of the unique features of ZTF is its frequent observations within 7° of the Galactic plane (see the spatial distribution of single-exposure epochs in DR1).[18] Previous all-sky surveys such as CRTS (Drake et al. 2014) generally avoided latitudes within 10° of the Galactic plane due to crowding and large pixel sizes. Exceptions include a few targeted surveys, such as the Optical Gravitational Lensing Experiment (OGLE), that were successful in finding large numbers of dwarf novae in the fields toward the Galactic Bulge and the Magellanic Clouds (Mroz et al. 2015) and the All Sky Automated Survey (ASAS) which had large pixels and a faint limit of only 14 mag (Pojmanski 1977). The 1″ pixels of ZTF allow the nightly plane observations to provide variable sources that can be identified in the Marshal. Figure 5 shows the distribution of Galactic latitudes for the objects in Tables 1 and 2. The number of objects lying within 10° of the Galactic plane confirm the higher densities expected there, albeit not as large as the numbers found from OGLE (likely due to the limitations expressed in Section 5). Of the previously identified CVs (Table 1), only 23 (26%) are within 10°, while among the strong candidates (Table 2), the number is 98 (45%) and 7 (33%) for the possible candidates in Table 3. While the more frequent sampling of the plane by ZTF maps the shape of outbursts better than the three-day sampling, the detection rates of outbursts should be about the same over the sky as dwarf nova outbursts normally last longer than 3 days. Thus, the summed number of known plus candidate systems (30–40 per 10° bin in the plane) compared to ⩽20 per bin out of the plane does imply a higher density of CVs, with most being new candidates.

[18] https://www.ztf.caltech.edu/page/dr1

3.3. Absolute Magnitudes

The available Gaia parallaxes (Gaia Collaboration 2018) provide distances that enable meaningful absolute magnitudes and heights above the plane without relying on average absolute magnitudes at quiescence or outburst. However, the

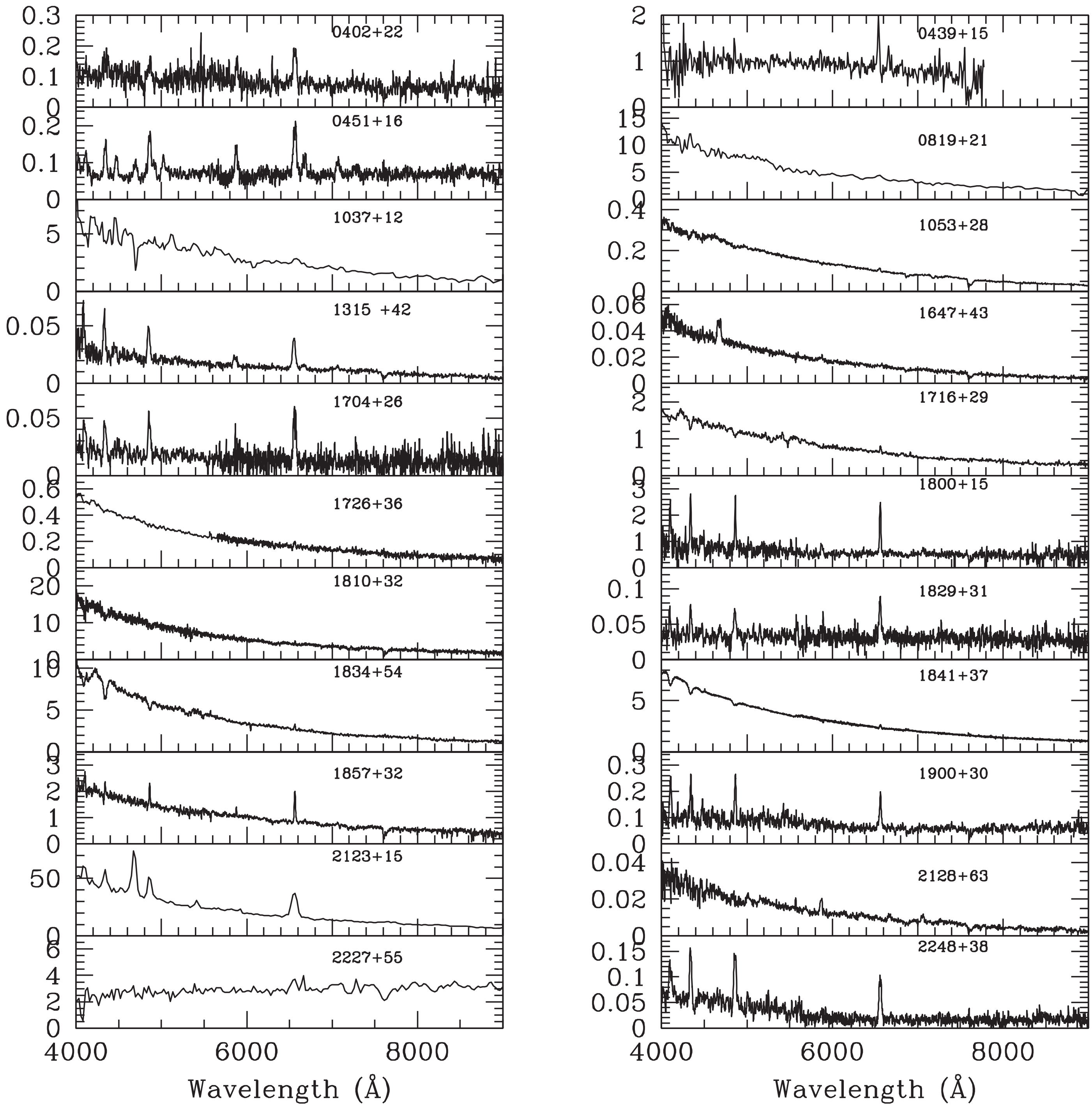

Figure 3. Blue and red spectra from Keck, Pal200in, WHT, APO, SEDM, and SPRAT showing at least one Balmer or Helium emission line. The vertical axis is F_λ in units of 10^{-16} erg cm^{-2} s^{-1} Å^{-1} except for the SPRAT spectrum of ZTF0439+15 which is normalized in its reduction procedure.

sample is small due to the current limits on the Gaia parallaxes. Table 1 (confirmed CVs) has 57 (63%) with good (S/N > 3) parallax measurements, while Table 2 has only 29 (13%) and Table 3 has 7 (33%). These numbers are consistent with the closest systems being found in previous discoveries and the new candidates having large distances and/or fainter brightness. Figure 6 plots the absolute magnitude of the objects from Tables 1 and 2. In the cases where ZTF did not get a detection for the quiescent magnitude, the upper limits mean that the absolute magnitudes will be even fainter than shown. Past results on absolute magnitudes of dwarf novae at quiescence (Warner 1987, 1995) have shown a range from 7.5 to 11, depending on the orbital period and the outburst recurrence time. Figure 6 shows that the majority of the ZTF sources are between 10 and 12, confirming that most systems are faint. To investigate whether ZTF is predisposed to a particular outburst type that would be related to mass transfer rate (such as the low mass transfer rate TOADS with infrequent, large amplitude outbursts; Howell et al. 1995), the absolute magnitudes are plotted versus detected outburst frequency in the interval covered by ZTF, in Figure 7 (top), as well as versus outburst amplitude (Figure 7 bottom). While the majority of the objects

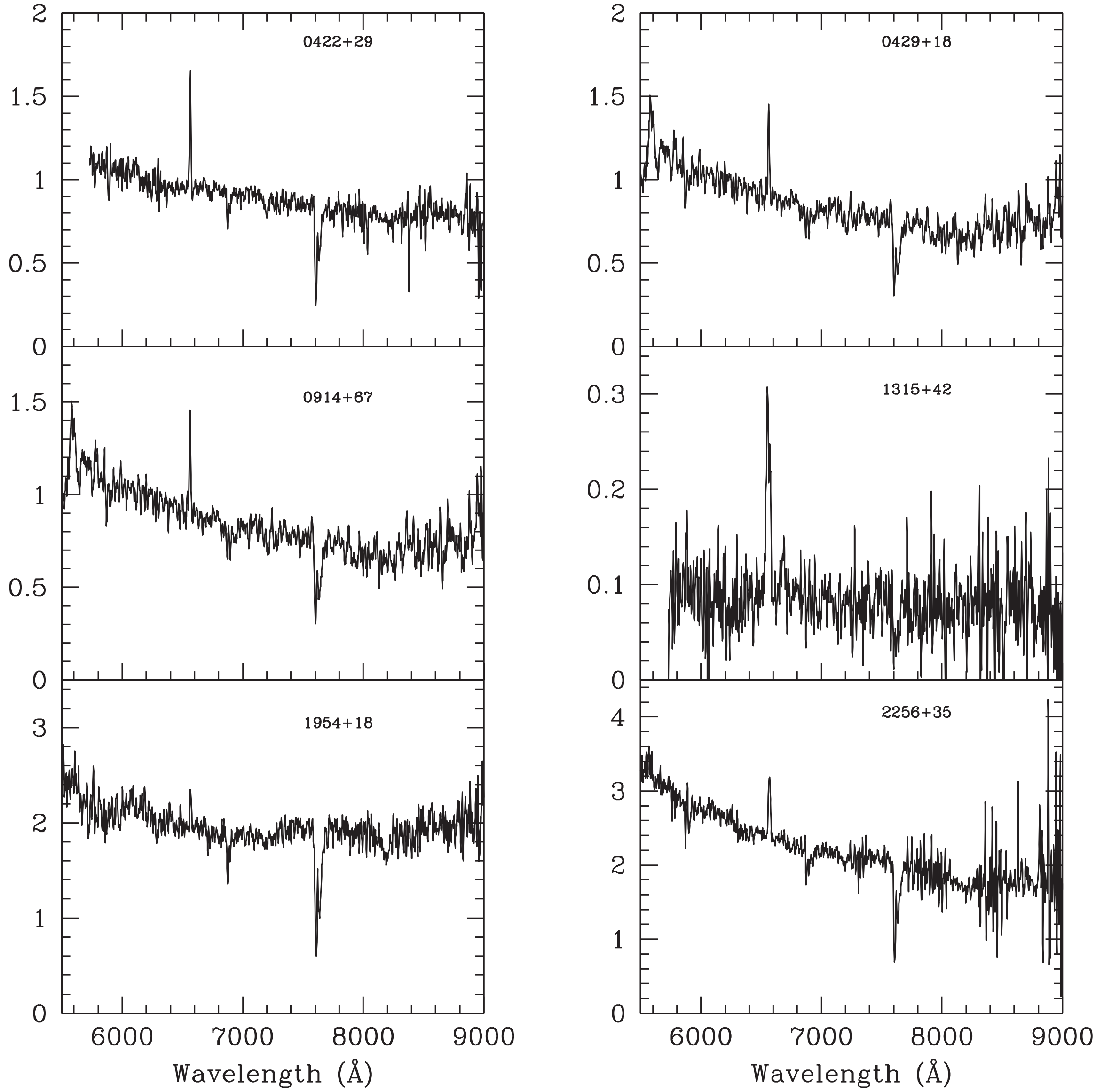

Figure 4. Red only spectra obtained at APO. The vertical axis is F_λ in units of 10^{-16} erg cm^{-2} s^{-1} Å^{-1}.

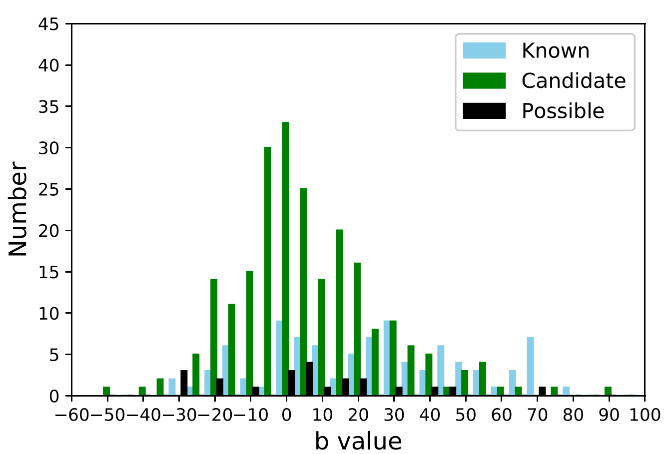

Figure 5. Number of systems in Tables 1–3 as a function of Galactic latitude (in 10 deg bins).

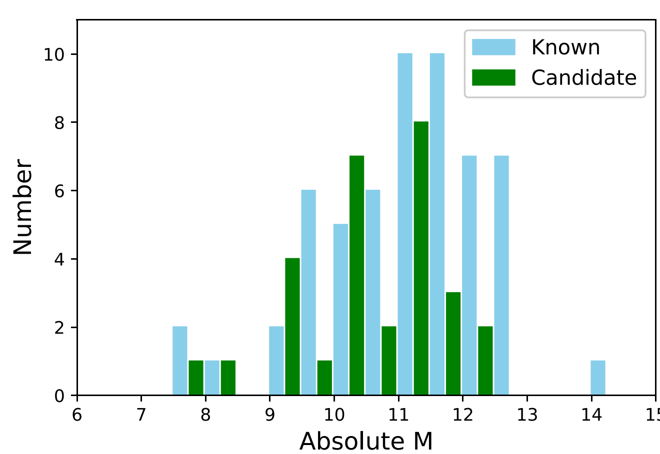

Figure 6. Number of systems in Tables 1 and 2 as a function of their absolute magnitude (in 0.5 mag bins) as determined from available Gaia parallaxes. Note that 5σ upper limits on the magnitudes for the fainter sources means that they are only brighter limits to the true absolute magnitude at quiescence.

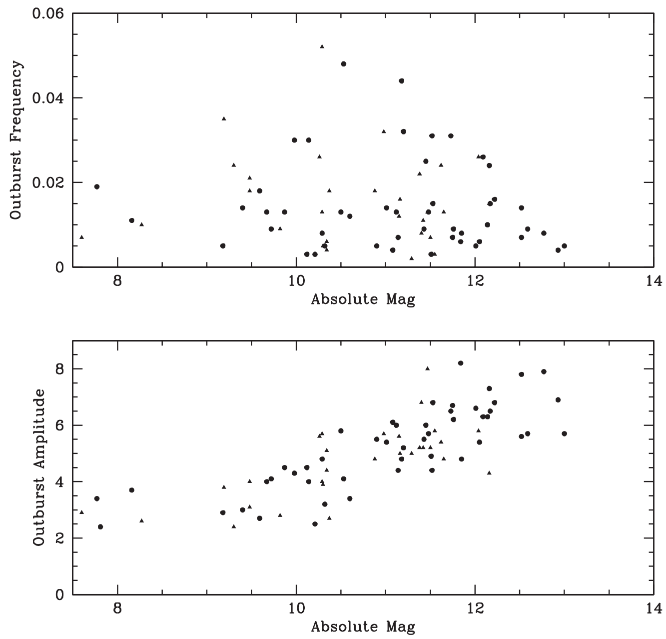

Figure 7. Plots of absolute magnitude vs. outburst frequency (top) and absolute magnitude vs. outburst amplitude (bottom) for the objects showing dwarf-nova-type outbursts in Table 1 (solid dots) and Table 2 (triangles).

have outburst frequencies less than 0.02 (50 days), there is a large scatter at all brightnesses. This result is consistent with those from smaller data sets (e.g., Howell et al. 1995; Thorstensen et al. 2002) that showed a wide range of outburst behavior for similar orbital periods and luminosities. However, the outburst amplitudes show a clear increase as the absolute magnitudes become fainter. Of the 14 objects fainter than 12th mag, 8 would qualify as candidates for TOADS (Howell et al. 1995), with outburst amplitudes $\geqslant$6 mag, and modeled by Howell et al. (1995) with low mass transfer and low disk viscosity. These eight are all in the previously known CVs (Table 1), while candidate CVs all have brighter absolute magnitudes. This is likely related to the low frequency of outbursts evident in this faint magnitude range (Figure 7 top) and the short timescale of the ZTF survey.

4. Notes on Individual Systems

Brief descriptions of the systems with interesting features in their spectra or light curves are provided below.

4.0.1. He II Objects

Figure 3 shows four systems from Table 2 with strong He II4686, or only helium lines, characteristics of AM CVn systems or those containing a magnetic white dwarf and/or very high accretion. ZTF2128+63 shows only lines of He and so is likely an AM CVn system. ZTF2123+15 has He II stronger than Hβ and a prominent blue continuum, making it a strong candidate for either an IP or a member of the class of high mass transfer rate NL called SW Sex stars (Thorsensen et al. 1991; Hoard et al. 1998) that have orbital periods between 3 and 4 hr. ZTF0451+16 also shows strong Balmer and He I lines as well as relatively strong He II, but without the blue continuum that is characteristic of a high mass accretion rate system, so is a candidate for a polar system. ZTF1647+43 is peculiar, as it has a very strong He II line and a very blue continuum but very weak Balmer emission. Further data are needed to refine its classification.

ZTF1631+69 (Table 1) has been identified as a CV (Appenzeller et al. 1998), and is reported in the ROSAT and XMM catalogs, but there is no detailed study of this system available in the literature. The ZTF light curve shows the existence of high and low states, a common feature of high accretion rate SW Sex systems as well as those containing highly magnetic white dwarfs (polars and IPs). A series of five sequential spectra obtained over the span of an hour at APO on 2019 May 24 shows strongly doubled Balmer lines along with He II, as well as large changes from one spectrum to the next (Figure 8). The velocities of the Hα and Hβ lines show a portion of a sinusoidal variation over 200 km s^{-1} during the hour but the time span is too short to determine an orbital period. The doubled lines are a signature of an accretion disk while the high excitation could indicate a magnetic white dwarf. Further data are needed to ascertain if this is an IP system.

4.0.2. Strong Balmer Lines

Figures 3 and 4 show that ZTF0422+29, ZTF0429+18, ZTF0439+18, ZTF0914+67, ZTF1315+42, ZTF1800+15, ZTF1704+26, ZTF1800+15, ZTF1829+31, ZTF1857+32, ZTF1900+30, and ZTF2248+38 all have the prominent Balmer emission lines typical of quiescent dwarf novae. ZTF0819+21, ZTF1037+12, ZTF1053+28, ZTF1716+29, ZTF1726+36, ZTF1810+32, ZTF1834+54, ZTF1841+37, ZTF1954+18, ZTF2227+55, and ZTF2256+35 show weak Hα in emission while the bluer Balmer lines are in absorption (for those with blue spectra as well as the red). The spectra of these systems were obtained close to their outburst brightness and reflect the prominence of the thick accretion disk at those times.

4.0.3. Peculiar Light Curves

ZTF1841+37 (Figure 1) shows an SOB followed by six normal outbursts or rebrightenings within 60 days. If this sequence repeats in future data, this could be a new ER UMa system. The cyclic behavior of SOBs interspersed with normal outbursts in this small group of CVs is thought to be a combination of a high mass transfer rate combined with a tidal instability present in short-period systems (Osaki 1996).

SIMBAD identifies ZTF1752+07 with V982 Oph and classifies it as a long-period variable candidate, but the ZTF light curve (Figure 9) and the blue colors at bright states are more consistent with a dwarf nova classification, as proposed by Antipin & Samus (2002).

5. Completeness

At this time, it is difficult to obtain a good estimate of how complete the Marshal is in finding all CVs. This first year was hampered by a late start of the Marshal filter, the loss of the month of October due to equipment improvements, significant weather losses in the winter months, and the lack of good reference images for all the fields. In addition, the CVs in any field may not have had a dwarf nova outburst or a change in low/high state during the months they were available in the sky. A rough estimate can be made using the results from SDSS spectra and the recent analysis of Pala et al. (2019) who used the overlap between Gaia and SDSS colors to determine the completeness of the CVs within 150 pc. The ∼300 available spectra from the SDSS Legacy

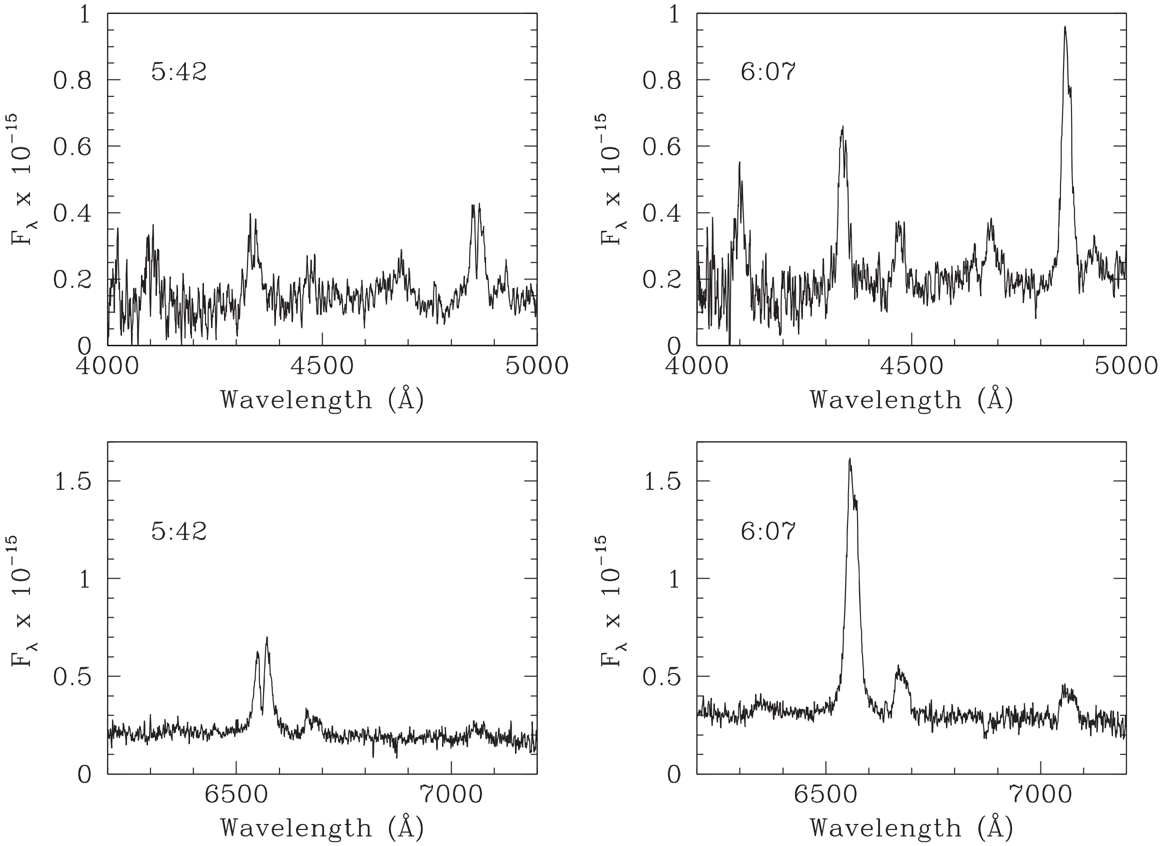

Figure 8. Two of the blue and red APO DIS spectra of 1631+69 obtained 25 minutes apart showing the large changes in the Balmer and He lines.

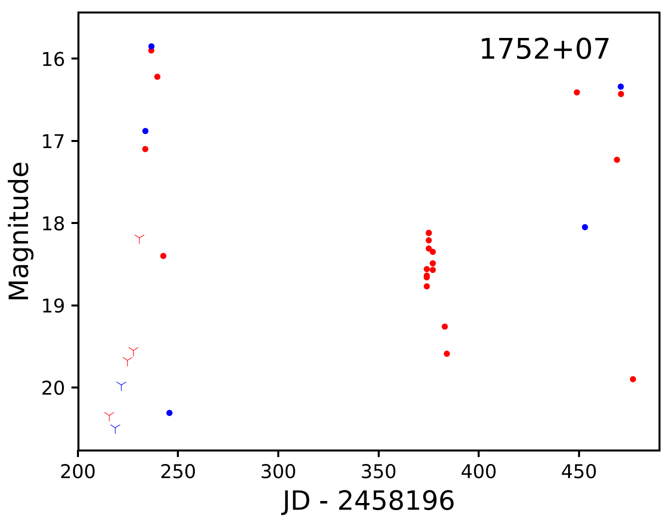

Figure 9. ZTF1752+07 (V982 Oph) light curve showing four dwarf-nova-type outbursts. Symbols are the same as those in Figure 1.

program provided a lower limit estimate of the density of CVs as 0.03 deg^{-2} (Szkody et al. 2003, 2011), and Pala et al. (2019) estimated that the spectral completeness of SDSS is ∼57%. ZTF covers about 62% of the sky (25,774 deg^2 so this should mean about 770 CVs should have been found, while only 308–329 were, which would be about 40% completeness). However, given the down time and weather, the actual usable time in the survey is probably closer to 6–9 months (390–580 CVs) which would be more like 53%–80%. Since the SDSS Legacy program was oriented toward high galactic latitudes to sample quasars, larger numbers for the stellar density are expected with the inclusion of low latitudes, so the lower percentages are likely more realistic. A better estimate will be possible as the survey proceeds and the lost months are re-observed and the reference fields are completed.

6. Conclusions

Using the GROWTH Marshal to filter nightly alerts from ZTF *g* and *r* light curves throughout the first year of operation resulted in the identification of 90 known CVs, 218 strong candidates based on the shape, amplitude and colors of the light curves, and an additional 21 potential candidates that require further data. Follow-up spectra obtained on a variety of 1.5–10 m telescopes allowed spectroscopic confirmation of 27 of the 218 strong candidates from Balmer emission lines, with an additional two with SDSS spectra. Unlike previous surveys, almost half of the new ZTF candidates are located within 10 degrees of the galactic plane, demonstrating the capability of the ZTF camera and software to discover objects in crowded fields. While only 13% of the strong candidates have available and significant Gaia parallaxes, most of their absolute magnitudes are consistent with the faint end of the CV distribution (10–12), similar to the CRTS. The outburst amplitudes increase with fainter absolute magnitudes in this range, with many of those fainter than 12 being good candidates for TOADs (Howell et al. 1995).

Four of the objects with spectra show high-excitation He II or only helium lines and deserve further time-resolved spectra to determine their correct classification as either a system containing a magnetic white dwarf or an SW Sex system, or an AM CVn type. Hour-long time-resolved spectra of the known CV ZTF1631+69 shows strong He II along with doubled Balmer emission lines, implying an IP origin. A previously identified long-period variable (V982 Oph) is more consistent with a dwarf nova classification as proposed by Antipin & Samus (2002).

While the available Marshal filter is not complete in finding all the CVs, it does demonstrate that even with several ongoing surveys, i.e., CRTS, ASASSN, and MASTER, there are many systems being missed, especially those in the Galactic plane. Completeness in any ground survey is difficult to obtain due to weather and software ability in crowded fields. Additionally, follow-up spectra of all the candidates is a time-consuming venture and will require increasingly large telescopes to obtain spectra at quiescent magnitudes. Unfortunately, classification is best near quiescence when the emission lines produce the most information from the intensity and shape as to the correct type of CV. Some compromise can be reached by obtaining observations midway from outburst to decline.

P.S. and B.D. acknowledge funding from NSF grant AST-1514737. A.Y.Q.H. is supported by a National Science Foundation Graduate Research Fellowship under grant No. DGE-1144469. M.C. is supported by the David and Ellen Lee Prize Postdoctoral Fellowship at the California Institute of Technology. M.L.G. acknowledges support from the DIRAC Institute in the Department of Astronomy at the University of Washington. The DIRAC Institute is supported through generous gifts from the Charles and Lisa Simonyi Fund for Arts and Sciences, and the Washington Research Foundation. We would like to thank occasional observers on the UW APO ZTF follow-up team, including Brigitta Sipőcz, James Davenport, Daniela Huppenkothen, Dino Bektešević Gwendolyn Eadie, and Bryce T. Bolin. The authors thank the Observatoire de la Côte d'Azur for support. This work was supported by the GROWTH project funded by the National Science Foundation under PIRE grant No. 1545949. Based on observations obtained with the Samuel Oschin Telescope 48 inch and the 60 inch Telescope at the Palomar Observatory as part of the Zwicky Transient Facility project. Z.T.F. is supported by the NSF under grant AST-1440341 and a collaboration including Caltech, IPAC, the Weizmann Institute for Science, the Oskar Klein Center at Stockholm University, the University of Maryland, the University of Washington, Deutsches Elektronen-Synchrotron and Humboldt University, Los Alamos National Laboratories, the TANGO Consortium of Taiwan, the University of Wisconsin at Milwaukee, and Lawrence Berkeley national Laboratories. Operations are conducted by COO, IPAC, and The SED Machine is based upon work supported by NSF under grant 1106171. Some observations were made with the Apache Point 3.5 m telescope, which is owned and operated by the Astrophysical Research Corporation. The Liverpool Telescope is operated on the island of La Palma by Liverpool John Moores University in the Spanish Observatorio del Roque de los Muchachos of the Instituto de Astrofisica de Canarias with financial support from the UK Science and Technology Facilities Council. The William Herschel Telescope is operated on the island of La Palma by the Isaac Newton Group of Telescopes in the Spanish Observatorio del Roque de los Muchachos of the Instituto de Astrofisica de Canarias.

Facilities: APO:3.5m, Hale, ING:Herschel, Keck:I, Liverpool:2m, PO:1.2m, PO:1.5m.

Note added in proof. F. Romanov (2020, private communication) reported that ZTF0117+58 has a spectrum in Verbeek et al. (2012), and thus merits being in Table 1 rather than Table 2.

ORCID iDs

Paula Szkody https://orcid.org/0000-0003-4373-7777
Brooke Dicenzo https://orcid.org/0000-0002-8257-9727
Anna Y. Q. Ho https://orcid.org/0000-0002-9017-3567
Jan van Roestel https://orcid.org/0000-0002-2626-2872
Melissa L. Graham https://orcid.org/0000-0002-9154-3136
Eric C. Bellm https://orcid.org/0000-0001-8018-5348
Kevin Burdge https://orcid.org/0000-0002-7226-836X
Thomas Kupfer https://orcid.org/0000-0002-6540-1484
Thomas A. Prince https://orcid.org/0000-0002-8850-3627
Frank J. Masci https://orcid.org/0000-0002-8532-9395
Przemyslaw J. Mróz https://orcid.org/0000-0001-7016-1692
Michael Coughlin https://orcid.org/0000-0002-8262-2924
Virginia A. Cunningham https://orcid.org/0000-0003-2292-0441
Matthew J. Graham https://orcid.org/0000-0002-3168-0139
David Kaplan https://orcid.org/0000-0001-6295-2881
Mansi M. Kasliwal https://orcid.org/0000-0002-5619-4938
Adam A. Miller https://orcid.org/0000-0001-9515-478X
Reed Riddle https://orcid.org/0000-0002-0387-370X
Maayane T. Soumagnac https://orcid.org/0000-0001-6753-1488

References

Antipin, S. V., & Samus, N. N. 2002, IBVS, 5302, 1
Appenzeller, I., Thiering, I., Zickgraf, F. J., et al. 1998, ApJS, 117, 319
Bellm, E. C., Kulkarni, S. R., Barlow, T., et al. 2019a, PASP, 131, 068003
Bellm, E. C., Kulkarni, S. R., Graham, M. J., et al. 2019b, PASP, 131, 018002
Benn, C., Dee, K., & Agocs, T. 2008, Proc. SPIE, 7014, 70146X
Blagorodnova, N., Neill, J. D., Walters, R., et al. 2018, PASP, 130, 035003
Breedt, E., Gänsicke, B. T., Drake, A. J., et al. 2014, MNRAS, 443, 3174
Drake, A. J., Djorgovski, S. G., Mahabel, A., et al. 2009, ApJ, 696, 870
Drake, A. J., Gänsicke, B. T., Djorgovski, S. G., et al. 2014, MNRAS, 441, 1186
Gaia Collaboration, Brown, A. G. A., Vallenari, A., et al. 2018, A&A, 616, A1
Graham, M. J., Kulkarni, S. R., Bellm, E. C., et al. 2019, PASP, 131, 078001
Hoard, D. W., Szkody, P., Still, M. D., Smith, R. C., & Buckley, D. A. H. 1998, MNRAS, 294, 689
Howell, S. B., Nelson, L. A., & Rappaport, S. 2001, ApJ, 550, 897
Howell, S. B., Rappaport, S., & Politano, M. 1997, MNRAS, 287, 929
Howell, S. B., Szkody, P., & Cannizzo, J. K. 1995, ApJ, 439, 337
Kasliwal, M. M., Cannella, C., Bagdasaryan, A., et al. 2019, PASP, 131, 038003
Lipunov, V., Kornilov, V., Gorbovskoy, E., et al. 2010, AdAst, 2010, 349171
Masci, F. J., Laher, R. R., Rusholme, B., et al. 2019, PASP, 131, 018003
Mroz, P., Udalski, A., Poleski, R., et al. 2015, AcA, 65, 313
Oke, J. B., Cohen, J. G., Carr, M., et al. 1995, PASP, 107, 375
Oke, J. B., & Gunn, J. E. 1982, PASP, 94, 586
Osaki, Y. , 1996, PASP, 108, 39
Pala, A., Gänsicke, B. T., Breedt, E., et al. 2019, MNRAS, in press (arXiv:1907.13152)
Pojmanski, G. 1977, AcA, 47, 467
Rigault, M., Neill, J. D., Blagoradnova, N., et al. 2019, A&A, 627, 115
Shappee, B. J., Prieto, J. L., Grupe, D., et al. 2014, ApJ, 788, 48
Steele, I. A., Smith, R. J., Rees, P. C., et al. 2004, Proc. SPIE, 5489, 679
Szkody, P., Anderson, S. F., Brooks, K., et al. 2011, AJ, 142, 181
Szkody, P., Fraser, O., Silvestri, N., et al. 2003, AJ, 126, 1499
Thorsensen, J. R., Ringwalkd, F. A., Wade, R. A., Schmidt, G. D., & Norsworthy, J. E. 1991, AJ, 102, 272
Thorstensen, J. R., Patterson, J., Kemp, J., & Vennes, S. 2002, PASP, 114, 1108
Verbeek, K., Groot, P. J., Scaringi, S., et al. 2012, MNRAS, 426, 1235
Warner, B. 1987, MNRAS, 227, 23
Warner, B. 1995, Cataclysmic Variable Stars (New York: Cambridge Univ. Press)
York, D. G., Adelman, J., Anderson, J. E., et al. 2000, AJ, 120, 1579